COMPUTER RESEARCH AND MODELING
2025 VOL. 17 NO. 1 P. 139–169
DOI: 10.20537/2076-7633-2025-17-1-139-169

Ки&М

ANALYSIS AND MODELING OF COMPLEX LIVING SYSTEMS

UDC: 519.876, 576.8, 517.9, 574.34

The impact of ecological mechanisms on stability in an eco-epidemiological model: Allee effect and prey refuge

T. Gaber[a], Widowati, R. Herdiana

Department of Mathematics, Faculty of Sciences and Mathematics, Diponegoro University, Semarang, 50275, Indonesia

E-mail: [a] taleb0gaber@gmail.com

Received 10.11.2024, after completion — 21.01.2025.
Accepted for publication 27.01.2025.

Eco-epidemiological models provide insights into factors influencing disease transmission and host population stability. This study developed two eco-epidemiological models to investigate the impacts of prey refuge availability and an Allee effect on dynamics. Model A incorporated these mechanisms, while model B did not. Both models featured predator – prey and disease transmission and were analyzed mathematically and via simulation. Model equilibrium states were examined locally and globally under differing parameter combinations representative of environmental scenarios. Model A and B demonstrated globally stable conditions within certain parameter ranges, signalling refuge and Allee effect terms promote robustness. Moreover, model A showed a higher potential toward extinction of the species as a result of incorporating the Allee effect. Bifurcation analyses revealed qualitative shifts in behavior triggered by modifications like altered predation mortality. Model A manifested a transcritical bifurcation indicating critical population thresholds. Additional bifurcation types were noticed when refuge and Allee stabilizing impacts were absent in model B. Findings showed disease crowding effect and that host persistence is positively associated with refuge habitat, reducing predator – prey encounters. The Allee effect also calibrated stability via heightened sensitivity to small groups. Simulations aligned with mathematical predictions. Model A underwent bifurcations at critical predator death rates impacting prey outcomes. This work provides a valuable framework to minimize transmission given resource availability or demographic alterations, generating testable hypotheses.

Keywords: Allee effect, prey refuge, predator – prey, eco-epidemiological model, nonlinear incidence rate, local stability, global stability, Hopf bifurcation, transcritical bifurcation

Citation: *Computer Research and Modeling*, 2025, vol. 17, no. 1, pp. 139–169.

1. Introduction

The dynamic interaction between predators and their prey is widely considered one of the most prevalent natural phenomena, as this relationship has become among the most extensively studied topics within ecology [Gaber, Herdiana, Widowati, 2024]. Prey shelters, harvesting, sickness, and the Allee effect are hugely impactful factors that can drastically alter the behaviors of predator – prey models, potentially producing very intriguing outcomes [Anggriani et al., 2023; Han, Dey, Banerjee, 2023; Kumar, Mandal, 2022; Li et al., 2022a; Li et al., 2022b; Molla et al., 2022; Pal et al., 2024; Shang, Qiao, 2024; Thirthar et al., 2022].

Studies from [Liang, Meng, 2023; Sen, Ghorai, Banerjee, 2019] demonstrated that incorporating prey refuge highly benefits ecological stability by decreasing interactions between hunter and hunted. There exist two standard forms of shelter: one where refuge size depends on prey numbers, with the rest vulnerable to capture. The other involves fixed refuge quantities. A steady Lotka – Volterra system remains unaffected by constant refuge. However, substantial refuge eliminates cycles, instead resulting in stable balances.

Typically, mathematical designs are employed to investigate the impacts of shelter on coupled population fluctuations, modeling predator – prey frameworks that include some manifestation of refuge safeguarding from predation [Al-Salti et al., 2021; Liu et al., 2021; Majeed, Ghafel, 2022; Sasmal, 2018; Vinoth et al., 2021], incorporating a fixed proportion of refuge alongside a Holling type II response function. Conversely, refuge correlating to interactions can instigate self-limitation within Lotka – Volterra's outcomes [Molla et al., 2022].

Additionally, the Allee effect may surface due to various natural phenomena such as lessened vigilance, inherited tendencies, mating troubles, and nutritional deficiencies at low densities c. [Cao, Ma, Hao, 2023] examined a changed Leslie – Gower model where prey growth aligned with a powerful multiplicative Allee effect governed by a Beddington – DeAngelis functional form. Numerous investigations likewise analyzed modified Leslie – Gower designs containing additive Allee effects using Holling type II response. [Pal, Pal, Chattopadhyay, 2018; Pal et al., 2019] found the Allee effect can heighten extinction risk. Thus, jointly exploring refuge's and Allee effects' impacts on predator – prey relational population behaviors may enhance comprehending conditions prompting species endangerment. Accordingly, we propose a predator – prey model combining two crucial components: 1) a Holling type II functional response depicting capture rates and 2) an additive Allee effect term influencing prey propagation. Integrating these elements will illuminate how Allee effects and refuge shape population fluctuations. Our suggested design intends offering a more inclusive and realistic representation of actual predator – prey interactions.

Furthermore, as predators' consuming histories affect the present birth rates, time delays emerge. Exploration has featured prey and predator delay designs alongside Allee effects. These lags dramatically impacted the design's security and behaviors, regularly prompting bifurcations and nonlinear phenomena. Accounting for such hold-ups provides a fuller characterization of real ecological interactions that inevitably involve utilitarian histories. Integrating time delays into our proposed predator – prey model containing Allee effects and refuge could yield supplemental comprehension of how delays interact with and amplify system intricacy elements. This defines an encouraging path for forthcoming research generating a highly nuanced and emblematic theoretical structure, [Anacleto, Vidal, 2020] supplied some insights on the existence of security commuting theoretically and probing bifurcation bearing concerning time delay. The nonlinear incidence rate was advanced by Gumel and Moghadas and adapted into our previous research [Gaber, Herdiana, Widowati, 2024] and used by numerous additional investigators [Kamrujjaman, Shahriar Mahmud, Islam, 2021; Lv, Ke, Li, 2020; Nabti, Ghanbari, 2021; Rohith, Devika, 2020], it is considered more precise than the straightforward mass action legislation when it comes to disease dispersing in parallel in types as it considers the crowding influence of the infected persons.

Our previous research [Gaber, Herdiana, Widowati, 2024] has focused on the dynamics of the predator – prey model with a nonlinear incidence rate where we noticed the occurrence of many transcritical bifurcations as well as a Hopf bifurcation.

In this paper, we go forward as we formulate a new eco-epidemiological model of a prey – predator with an infection in the prey population following a nonlinear incidence rate just as in [Gaber, Herdiana, Widowati, 2024] adding the Allee effect using a different term than the one used in [Molla et al., 2022] and a prey refuge which is only proportional to the prey as hideouts like tree limbs, caverns, and camouflage. Our proposed model adheres to Holling type II responsiveness in vulnerable-prey and predator interactions and fundamental mass action legislation in contaminated prey – predator interplay, designed to better depict infection weakening exposed prey incapable of sheltering or fleeing. We cover crowded infected-individual impacts assuming disease transmission amongst vulnerable and infected prey resulting from contact as stated by the nonlinear incidence rate.

To illustrate the applicability of our model, we draw on the real-world example of *Toxoplasma gondii* infections in rodent populations and their interactions with feline predators [Berdoy, Webster, Macdonald, 2000]. Infected rodents exhibit altered behaviors, such as reduced aversion to predators, which increases their susceptibility to predation. This behavioral shift enhances parasite transmission to definitive hosts, such as cats [Flegr, 2007]. The dynamics observed in this system align with the theoretical constructs of our model, particularly the differential predation rates and the influence of disease on prey vulnerability. Including such examples demonstrates the relevance and realism of the proposed eco-epidemiological framework.

2. The mathematical model

An eco-epidemiological simulation is comprised of prey and predator populations. The prey is split into susceptible (S) and infected (I) groups. The predators are considered continually healthy. We will follow the following assumptions in building our model:

1. Initially, without disease, prey numbers follow a logistical curve of limited growth towards the environment's carrying capacity (K), fueled by a reproductive rate (α).

2. Two prey classifications exist: susceptible $S(t)$ and infected $I(t)$. Susceptibles alone breed, allowing replenishment to K. Infecteds lack reproduction and resource competition during illness. This realistically portrays functionality reductions when diseased.

3. Transmission between S and I employs a nonlinear incidence rate of $\frac{\beta IS}{1+I}$ proposed by Gumel and Moghadas [Gaber, Herdiana, Widowati, 2024]. βI represents infection pressure from the infected, while $\frac{1}{1+I}$ incorporates hindrances from crowded infected.

4. Predators consume both prey classes equally.

5. Infected prey weakened state allows swift consumption, so handling time approaches zero, simplifying to a Holling type I functional response.

6. Healthy prey faces a Holling type II response.

7. Resources only aid susceptible, with infected excluded due to illness. Moreover, infected evade capacity constraints unlike susceptible experiencing Allee effects.

First let us construct the model without Allee and refuge effects, and considering the above-mentioned assumptions the model becomes:

$$\begin{aligned} \frac{dS}{dT} &= \alpha S\left(1-\frac{S}{K}\right)-\frac{\beta S I}{1+I}-\frac{m_1 S P}{h+S}, \\ \frac{dI}{dT} &= \frac{\beta S I}{1+I}-m_2 I P-d_1 I, \\ \frac{dP}{dT} &= \frac{e_1 m_1 S P}{h+S}+e_2 m_2 I P-d_2 P. \end{aligned} \tag{1}$$

Adding the Allee effect under assumption number 7:

$$\begin{aligned} \frac{dS}{dT} &= \alpha S\left(1-\frac{S}{K}\right)\left(\frac{S}{k_0}-1\right)-\frac{\beta S I}{1+I}-\frac{m_1 S P}{h+S}, \\ \frac{dI}{dT} &= \frac{\beta S I}{1+I}-m_2 I P-d_1 I, \\ \frac{dP}{dT} &= \frac{e_1 m_1 S P}{h+S}+e_2 m_2 I P-d_2 P. \end{aligned} \tag{2}$$

Now by adding the refuge effect under assumption number 7 we get the model with the prey refuge and Allee effect:

$$\begin{aligned} \frac{dS}{dT} &= \alpha S\left(1-\frac{S}{K}\right)\left(\frac{S}{k_0}-1\right)-\frac{\beta S I}{1+I}-\frac{m_1(1-n) S P}{h+(1-n)S}, \\ \frac{dI}{dT} &= \frac{\beta S I}{1+I}-m_2 I P-d_1 I, \\ \frac{dP}{dT} &= \frac{e_1 m_1(1-n) S P}{h+(1-n)S}+e_2 m_2 I P-d_2 P. \end{aligned} \tag{3}$$

Here all the parameters are assumed to be positive constants.

Our suggested design intends offering a more inclusive and realistic representation of actual predator – prey interactions. The behavioral dynamics observed in *Toxoplasma gondii* infections provide a concrete example that reflects the assumptions in our models. For instance, the altered behavior of infected prey leading to increased predation rates demonstrates how disease dynamics can influence population interactions and stability. This real-world example validates the inclusion of mechanisms such as differential predation and prey vulnerability, reinforcing the ecological relevance of our framework. Additionally, examples of the Allee effect and prey refuge effect further support the assumptions and outcomes of our models. For instance, the Allee effect is evident in African wild dog (*Lycaon pictus*) populations, where group hunting efficiency and defense mechanisms decline as population sizes drop, leading to lower survival rates [Courchamp, Clutton-Brock, Grenfell, 2000]. Similarly, Huffaker's mite experiments demonstrated how introducing spatial refuges for prey species significantly stabilized predator – prey dynamics [Hupfaker, 1958]. Furthermore, the crowding effect of infected prey can be observed in amphibian populations impacted by chytrid fungus (Batrachochytrium dendrobatidis), where high densities lead to increased transmission rates and accelerated population declines [Catenazzi et al., 2011]. These examples underscore the robustness and applicability of our proposed eco-epidemiological models, aligning theoretical constructs with real-world observations.

3. The dimensionless form of the model

In this section a parameter reduction is pursued by deriving dimensionless representations of the model, simplifying the analysis.

Let's assume that:

$$sK = S, \quad iK = I, \quad pK = P, \quad T = \frac{t}{\alpha}.$$

Now we substitute into (1) and (3).

System (1) which is without Allee effect nor Prey refuge referred to as model B becomes:

$$\begin{aligned} \frac{ds}{dt} &= s(1-s) - \frac{a_2 si}{a_3 + i} - \frac{b_1 sp}{c_1 + s}, \\ \frac{di}{dt} &= \frac{a_2 si}{a_3 + i} - b_2 ip - c_2 i, \\ \frac{dp}{dt} &= \frac{e_1 b_1 sp}{c_1 + s} + e_2 b_2 ip - c_3 p. \end{aligned} \tag{4}$$

System (3) which is includes Allee effect and Prey refuge referred to as model A becomes:

$$\begin{aligned} \frac{ds}{dt} &= s(1-s)(a_1 s - 1) - \frac{a_2 si}{a_3 + i} - \frac{b_1(1-n)sp}{c_1 + (1-n)s}, \\ \frac{di}{dt} &= \frac{a_2 si}{a_3 + i} - b_2 ip - c_2 i, \\ \frac{dp}{dt} &= \frac{e_1 b_1 (1-n)sp}{c_1 + (1-n)s} + e_2 b_2 ip - c_3 p, \end{aligned} \tag{5}$$

where $a_1 = \frac{K}{k_0}$, $a_2 = \frac{\beta}{\alpha}$, $a_3 = \frac{1}{K}$, $b_1 = \frac{m_1}{\alpha}$, $b_2 = \frac{m_2 K}{\alpha}$, $c_1 = \frac{h}{k}$, $c_2 = \frac{d_1}{\alpha}$, $c_3 = \frac{d_2}{\alpha}$ and $a_1, a_2, a_3, b_1, b_2, c_1, c_2, c_3 > 0$.

Moving on we will study two models: model A and model B.

4. Positivity and boundedness

In this section, establishing the model's well-posed is the aim, by verifying positivity and boundedness.

4.1. Existence and uniqueness of the solution for model A

Theorem 1. *For system* (5) *with initial conditions* $s(0)$, $i(0)$, $p(0)$ *greater than or equal to zero, all solutions exist uniquely over the finite time interval* $[0, \xi]$ *where* $0 < \xi < \infty$. *Furthermore, the solutions* $s(t)$, $i(t)$, $p(t)$ *remain greater than or equal to zero throughout this period.*

$$s(0) = s_0 \geqslant 0, \quad i(0) = i_0 \geqslant 0, \quad p(0) = p_0 \geqslant 0, \quad t \geqslant 0. \tag{6}$$

Proof. From (5) we write:

$$\begin{aligned} \frac{ds}{dt} &= s(1-s)(a_1 s - 1) - \frac{a_2 si}{a_3 + i} - \frac{b_1(1-n)sp}{c_1 + (1-n)s} = g_1(x), \\ \frac{di}{dt} &= \frac{a_2 si}{a_3 + i} - b_2 ip - c_2 i = g_2(x), \\ \frac{dp}{dt} &= \frac{e_1 b_1 (1-n)sp}{c_1 + (1-n)s} + e_2 b_2 ip - c_3 p = g_3(x). \end{aligned} \tag{7}$$

The phase space for the system (7) is

$$R^3_+ = \left\{(s,\, i,\, p) \in R^3 :\ s \geqslant 0,\ i \geqslant 0,\ p \geqslant 0\right\}.$$

Given that the functions $f_1(x)$, $f_2(x)$, $f_3(x)$ defining the system are continuous on R^3; therefore, these functions are Lipschitzian on R^3_+ with continuous partial derivatives, they satisfy the Lipschitz condition on the nonnegative phase space R^3_+. Therefore, according to theorems regarding the existence and uniqueness of solutions for differential equations [Gaber, Herdiana, Widowati, 2024] the system defined by equation (7) under the nonnegative initial condition specified in (6) will possess a single solution that is defined on the interval $[0, \varepsilon]$ for any epsilon choice where $0 < \varepsilon < \infty$. In other words, given the regularity properties of the functions governing the system dynamics, there exists a unique trajectory satisfying the initial value problem over any finite time horizon. Integrating (7) with respect to initial conditions, we get

$$\begin{aligned} s(t) &= s(0)e^{\int_0^t g_1(s(x), i(x), p(x))\,dx} \geqslant 0, \\ i(t) &= i(0)e^{\int_0^t g_2(s(x), i(x), p(x))\,dx} \geqslant 0, \\ p(t) &= p(0)e^{\int_0^t g_3(s(x), i(x), p(x))\,dx} \geqslant 0. \end{aligned} \tag{8}$$

This proves the theorem. □

4.2. Uniformly boundedness of model A

The bounded nature suggests that our model comports well with biological principles. The limited scope of the system, as defined by equation (5), is proven via Theorem 2.

Theorem 2. *All solutions originating within the positive x-axis cube remain uniformly bounded.*

Proof. The proof considers two initial s value scenarios.

Case 1: Let $s(0) \leqslant 1$ and we claim $s(t) \leqslant 1$.

We prove by contradiction; let's assume $s(t) \geqslant 1$, then $\exists t_1, t_2$ such that $s(t_1) = 1$ and $s(t_2) > 1$ then $\forall t \in (t_1, t_2]$ we say $s(t) > 1$ is true.

From (10) we can write

$$\begin{aligned} s(t) = s(0)e^{\int_0^t f_1(s(x), i(x), p(x))\,dx} &= s(0)e^{\int_0^{t_1} f_1(s(x), i(x), p(x))\,dx + \int_{t_1}^t f_1(s(x), i(x), p(x))\,dx}, \\ s(t) &= s(t_1)e^{\int_{t_1}^t f_1(s(x), i(x), p(x))\,dx}. \end{aligned} \tag{9}$$

We have $s(t_1) = 1$. Then (9) becomes:

$$s(t) = e^{\int_{t_1}^t f_1(s(x), i(x), p(x))\,dx}, \tag{10}$$

but $s(t) > 1$ as in our assumption and

$$f_1(s(t), i(t), p(t)) = s(t)(1 - s(t))(a_1 s(t) - 1) - \frac{a_2 s(t) i(t)}{a_3 + i(t)} - \frac{b_1(1 - n)s(t)p(t)}{c_1 + (1 - n)s} < 0. \tag{11}$$

$a_1 > 1$ and $s(t) > 1$ as in our assumption, then $f_1(t) < 0$. Going back to (10), we find $s(t) < 1$, contradiction.

Case 2: Let $s(0) > 1$ and we claim $\limsup_{t\to\infty} s(t) \leqslant 1$.

Suppose it is not true. Then $s(t) > 1$ and $\forall t > 0$ and so $f_1(t) < 0$.

From l_1 we have:

$$\frac{ds}{dt} = s(1-s)(a_1 s - 1) - \frac{a_2 si}{a_3 + i} - \frac{b_1(1-n)sp}{c_1 + (1-n)s}, \tag{12}$$

since $s(t) > 1$, it follows that

$$\frac{ds}{dt} < s(1-s)(a_1 s - 1) \leqslant s(1-s)(a_1 \underline{s} - 1) < (1-s) \quad \text{where } \underline{s} = \lim_{t\to\infty} \inf s(t). \tag{13}$$

Integrating (13) and letting $t \to \infty$, we get $s(t) < 1$ when $t \to \infty$, a contradiction. Hence, $\lim\limits_{t\to\infty} \sup s(t) \leqslant 1$.

It suffices to demonstrate that the cumulative population, denoted by w and encompassing susceptible, infected, and predator components, remains bounded at all t above zero. Equation (14) represents the derivative of Γ:

$$w' = s' + i' + p' \quad \text{where } ' = \frac{d}{dt}. \tag{14}$$

From (14) we have

$$w' = s(1-s)(a_1 s - 1) - \frac{b_1(1-n)sp}{c_1 + (1-n)s}(1-e_1) - b_2 ip(1-e_2) - c_2 i - c_3 p \leqslant s(1-s)(a_1 s - 1) - c_2 i - c_3 p$$

we take $\mu = \min\{c_2, c_3\}$. Then:

$$\begin{aligned} w' + \mu w &\leqslant s(1-s)(a_1 s - 1) - c_2 i - c_3 p + \mu(s + i + p) \leqslant \\ &\leqslant s(1-s)(a_1 s - 1) - c_2 i - c_3 p + \mu(s + i + p) \leqslant s[(1-s)(a_1 s - 1) + \mu] - (c_2 - \mu)i - (c_3 - \mu)p \leqslant \\ &\leqslant s[(1-s)(a_1 s - 1) + \mu] \leqslant s(-a_1 s^2 + (a_1 + 1)s - 1) + \mu s \leqslant \\ &\leqslant -a_1 s\left(s^2 - \frac{a_1 + 1}{a_1}s + \left(\frac{a_1 + 1}{2a_1}\right)^2\right) - (1-\mu)s + a_1 s\left(\frac{a_1 + 1}{2a_1}\right)^2 \leqslant a_1 s\left(\frac{a_1 + 1}{2a_1}\right)^2, \end{aligned}$$

where $0 \leqslant s \leqslant 1$,

$$w' + \mu w \leqslant a_1\left(\frac{a_1 + 1}{2a_1}\right)^2 = \theta \quad \text{constant},$$

$$w' + \mu w \leqslant \theta \implies w' \leqslant \theta - \mu w.$$

Following the theory of differential inequality, we obtain

$$0 < w < w(0)e^{-\mu t} - \frac{\theta}{\mu}e^{-\mu t} + \frac{\theta}{\mu}, \tag{15}$$

where $w(0)$ denotes the initial value of the total population.

Now for $t \to \infty$ in (15) we get $w < \frac{\theta}{\mu}$,

$$w < \frac{a_1}{\mu}\left(\frac{a_1 + 1}{2a_1}\right)^2. \tag{16}$$

The information provided suggests that the overall population size $w(t)$ which is described by the function f has an upper limit as time increases towards infinity. Specifically, the source material indicates that $w(0)$ at the initial time $t = 0$ is bounded by the value $\frac{a_1}{\mu}\left(\frac{a_1+1}{2a_1}\right)^2$ as the time t grows

to infinity. By considering equations (15) and (16) together, one can thus conclude that the total population $w(t)$ is bounded as

$$0 \leqslant w(t) \leqslant \frac{a_1}{\mu}\left(\frac{a_1+1}{2a_1}\right)^2. \tag{17}$$

As in (17), we can confirm that $\frac{a_1}{\mu}\left(\frac{a_1+1}{2a_1}\right)^2$ is an upper bound of $w(t)$. Therefore, the feasible solution for our system (6) stays in the positively invariant region Ω, where $\Omega = \left\{(s, i, p) \in R_+^3 : w \leqslant \frac{a_1}{\mu}\left(\frac{a_1+1}{2a_1}\right)^2 + \xi \ \forall \xi > 0\right\}$. □

The bounded nature suggests that our model comports well with biological principles. The limited scope of the system, as defined by equation (5), is proven via Theorem 2. In this theorem, we demonstrate that all population sizes remain uniformly bounded, ensuring biological plausibility. Real-world systems, such as the predator – prey dynamics influenced by *Toxoplasma gondii*, align with this boundedness. The parasite-induced behavioral changes in prey populations illustrate the impact of disease on stability and predator – prey interactions. Incorporating features such as prey refuge and disease crowding effects further enhances the model's robustness and its ability to mirror realistic dynamics. In conclusion, we can confirm that the system defined by equation (5) has both biological relevance and sound mathematical properties within the specified domain Ω.

5. Equilibrium analysis of model A

Here we will calculate the equilibrium points of model A and check their feasibility conditions.

5.1. Equilibrium points

Now using the Maple tool, we acquire the equilibrium points of the system in (5).

The system (5) has the following equilibrium points:

1. The trivial equilibrium point $E_0(0, 0, 0)$.
2. The axial equilibrium points $E_1(1, 0, 0)$, $E_2\left(\frac{1}{a_1}, 0, 0\right)$.
3. The susceptible prey free equilibrium point (s-free equilibrium point) $E_3 = \left(0, \frac{c_3}{e_2 b_2}, -\frac{c_2}{b_2}\right)$.
4. The disease-free equilibrium point (i-free equilibrium point) $E_4(\overline{s}, 0, \overline{p})$,

$$\overline{s} = \frac{c_1 c_3}{(b_1 e_1 - c_3)(1-n)},$$

$$\overline{p} = \frac{e_1 c_1}{(b_1 e_1 - c_3)^3 (n-1)^3}(a_1 c_1 c_3 + (b_1 e_1 - c_3)(n-1))(c_1 c_3 + (b_1 e_1 - c_3)(n-1)).$$

The predator-free equilibrium points (p-free equilibrium points) $E_5(s^*, i^*, 0)$, where

$$s^* = \frac{c_2}{a_2}\left(a_3 + \text{the roots of the cubic equation } \left(v_3 z^3 + v_2 z^2 + v_1 z + v_0\right)\right),$$

i^* is the positive roots of the cubic equation $\left(v_3 z^3 + v_2 z^2 + v_1 z + v_0\right) v_3 = a_1 c_2^2$, $v_2 = 3u_1 - u_2$, $u_1 = a_1 a_3 c_2^2$, $u_2 = a_2 c_2 (a_1 + 1)$, $v_1 = a_3(3u_1 - 2u_2) + a_2^2(a_2 + 1)$, $v_0 = a_3^2(u_1 - u_2) + a_3 a_2^2$.

5. Interior equilibrium points $\widetilde{E}(\widetilde{s}, \widetilde{i}, \widetilde{p})$, $\widetilde{s} = \frac{Q}{G}$, $\widetilde{i}$ are the positive roots of the equation $\left(H_4Z^4 + H_3Z^3 + H_2Z^2 + H_1Z + H_0\right)$,

$$\widetilde{p} = -a_3b_2c_2e_2 * \left(\text{the negative roots of the equation } \left(L_4Z^4 + L_3Z^3 + L_2Z^2 + L_1Z + L_0\right)\right),$$

where

$$Q = \left(b_2e_2 * \left(\text{the roots of the equation } \left(Q_4Z^4 + Q_3Z^3 + Q_2Z^2 + Q_1Z + Q_0\right)\right) - c_3\right)c_1,$$
$$G = \left(b_2e_2 * \left(\text{the roots of the equation } \left(G_4Z^4 + G_3Z^3 + G_2Z^2 + G_1Z + G_0\right)\right) + e_1b_1 - c_3\right)(n-1).$$

5.2. Feasibility for model A equilibria

It is clear that equilibria E_0, E_1, E_2 are feasible, while E_3 is not feasible, so a further analysis is not necessary, E_4 satisfies feasibility conditions under $c_3 < b_1e_1$ and $c_1c_3 < (b_1e_1 - c_3)(1-n) < a_1c_1c_3$ to verify existence of $E_5\,(s^*, i^*, 0)$ which represents a predator-free state (p-free equilibrium points), one can examine the nonlinear algebraic system defined by

$$\begin{gathered} s(1-s)(a_1s-1) - \frac{a_2si}{a_3+i} - \frac{b_1(1-n)sp}{c_1+(1-n)s} = 0, \\ \frac{a_2si}{a_3+i} - b_2ip - c_2i = 0, \\ \frac{e_1b_1(1-n)sp}{c_1+(1-n)s} + e_2b_2ip - c_3p = 0, \end{gathered} \tag{18}$$

where s^*, $i^* > 0$ and $p^* = 0$.

Substituting $s = s^*$, $i = i^*$ and $p = 0$ into the system (18), we get

$$\begin{gathered} s^*(1-s^*)\left(a_1s^*-1\right) - \frac{a_2s^*i^*}{a_3+i^*} = 0, \\ \frac{a_2s^*i^*}{a_3+i^*} - c_2i^* = 0. \end{gathered} \tag{19}$$

By summing equations (19),

$$\begin{gathered} s^*(1-s^*)\left(a_1s^*-1\right) - c_2i^* = 0, \\ i^* = \frac{s^*(1-s^*)\left(a_1s^*-1\right)}{c_2}. \end{gathered} \tag{20}$$

But $i^* > 0$, then

$$\begin{gathered} \frac{s^*(1-s^*)\left(a_1s^*-1\right)}{c_2} > 0, \\ s^*(1-s^*)\left(a_1s^*-1\right) > 0. \end{gathered} \tag{21}$$

Therefore, E_5 is feasible under the condition $\frac{1}{a_1} < s^* < 1$ and $\frac{1}{c_2a_1} < i^* < \frac{1}{c_2}$ and $a_1 > 1$.

For the interior equilibrium point $\widetilde{E}(\widetilde{s}, \widetilde{i}, \widetilde{p})$ is feasible if and only if there is a solution where $\widetilde{s}, \widetilde{i}, \widetilde{p} > 0$ to the following algebraic nonlinear system:

$$\widetilde{s}(1-\widetilde{s})(a_1\widetilde{s}-1) - \frac{a_2\widetilde{s}\,\widetilde{i}}{a_3+\widetilde{i}} - \frac{b_1(1-n)\widetilde{s}\,\widetilde{p}}{c_1+(1-n)\widetilde{s}} = 0, \tag{r_1}$$

$$\frac{a_2\widetilde{s}\,\widetilde{i}}{a_3+\widetilde{i}} - b_2\widetilde{i}\,\widetilde{p} - c_2\widetilde{i} = 0, \tag{r_2}$$

$$\frac{e_1b_1(1-n)\widetilde{s}\,\widetilde{p}}{c_1+(1-n)\widetilde{s}} + e_2b_2\widetilde{i}\,\widetilde{p} - c_3\widetilde{p} = 0. \tag{r_3}$$

From (r_3) we get

$$\widetilde{i} = \frac{1}{e_2b_2}\left(c_3 - \frac{e_1b_1(1-n)\widetilde{s}}{c_1+(1-n)\widetilde{s}}\right). \tag{22}$$

When $\widetilde{i} > 0$, if $c_3 < b_1e_1$ then (22) can be written as

$$\widetilde{s} < \frac{c_1c_3}{(1-n)(e_1b_1-c_3)}. \tag{23}$$

If $c_3 > b_1e_1$ then (22) can be written as

$$\widetilde{s} > \frac{c_1c_3}{(1-n)(e_1b_1-c_3)}. \tag{24}$$

From (r_2) we get

$$\widetilde{p} = \frac{a_2\widetilde{s}}{b_2(a_3+\widetilde{i})} - \frac{c_2}{b_2}, \tag{25}$$

if $\widetilde{p} > 0$, then (25) becomes

$$\widetilde{i} < \frac{a_2\widetilde{s}-a_3c_2}{c_2}, \quad \widetilde{s} > \frac{a_3c_2}{a_2}. \tag{26}$$

Therefore, $\widetilde{E}$ is feasible under either the conditions

$$\widetilde{s} > \max\left\{\frac{a_3c_2}{a_2}, \frac{c_1c_3}{(1-n)(e_1b_1-c_3)}\right\}, \tag{27}$$

when $c_3 > b_1e_1$ and $0 < \widetilde{i} < \frac{a_2\widetilde{s}-a_3c_2}{c_2}$, or

$$\frac{a_3c_2}{a_2} < \widetilde{s} < \frac{c_1c_3}{(1-n)(e_1b_1-c_3)}, \tag{28}$$

when $c_3 < b_1e_1$ and $0 < \widetilde{i} < \frac{a_2\widetilde{s}-a_3c_2}{c_2}$.

6. Stability analysis

The terminology "LAS" will be employed rather than "locally asymptotically stable" for brevity. Determining LAS properties involves linearizing the system around each equilibrium and analyzing the corresponding Jacobian matrix. Equilibria where all eigenvalues have negative real parts or the one that satisfies the Routh Hurwitz criterion will be classified as LAS, indicating the ability to withstand minor fluctuations and return to equilibrium.

Local stability analysis of model A

The Jacobean matrix for the system (5),

$$J = \begin{pmatrix} a_{1,1} & a_{1,2} & a_{1,3} \\ a_{2,1} & a_{2,2} & a_{2,3} \\ a_{3,1} & a_{3,2} & a_{3,3} \end{pmatrix},$$

$$a_{1,1} = -3a_1 s^2 + 2(a_1+1)s - 1 - \frac{a_2 i}{a_3 + i} - \frac{b_1(1-n)p}{c_1 + (1-n)s} + \frac{b_1(1-n)^2 sp}{(c_1 + (1-n)s)^2},$$

$$a_{1,2} = -\frac{a_2 s}{a_3 + i} + \frac{a_2 si}{(a_3+i)^2}, \quad a_{1,3} = -\frac{b_1(1-n)s}{c_1 + (1-n)s}, \quad a_{2,1} = \frac{a_2 i}{a_3 + i},$$

$$a_{2,2} = \frac{a_2 s}{a_3 + i} - \frac{a_2 si}{(a_3+i)^2} - b_2 p - c_2, \quad a_{2,3} = -b_2 i, \quad a_{3,1} = \frac{e_1 b_1 (1-n)p}{c_1 + (1-n)s}\left(1 - \frac{(1-n)s}{c_1 + (1-n)s}\right),$$

$$a_{3,2} = e_2 b_2 p, \quad a_{3,3} = \frac{e_1 b_1 (1-n)s}{c_1 + (1-n)s} + e_2 b_2 i - c_3.$$

Now we analyze around each equilibrium point.

Around $E_0(0, 0, 0)$:

$$J_0 = \begin{pmatrix} -1 & 0 & 0 \\ 0 & -c_2 & 0 \\ 0 & 0 & -c_3 \end{pmatrix},$$

and the eigenvalues are $\lambda_1 = -1$, $\lambda_2 = -c_2$, $\lambda_3 = -c_3$ since $c_2, c_3 > 0$ all negative real numbers $\Rightarrow$ E_0 is LAS.

Around $E_1(1, 0, 0)$:

$$J_1 = \begin{pmatrix} 1 - a_1 & -\frac{a_2}{a_3} & -\frac{b_1(1-n)}{c_1+1-n} \\ 0 & \frac{a_2}{a_3} - c_2 & 0 \\ 0 & 0 & \frac{e_1 b_1(1-n)}{c_1+1-n} - c_3 \end{pmatrix},$$

and the eigenvalues are $\lambda_1 = 1 - a_1$, $\lambda_2 = \frac{a_2}{a_3} - c_2$, $\lambda_3 = \frac{e_1 b_1(1-n)}{c_1+1-n} - c_3$. $\lambda_1 < 0$ if $1 - a_1 < 0 \Rightarrow a_1 > 1$, $\lambda_2 < 0$ if $\frac{a_2}{a_3} - c_2 < 0 \Longrightarrow c_2 > \frac{a_2}{a_3}$, $\lambda_3 < 0$ if $\frac{e_1 b_1(1-n)}{c_1+1-n} - c_3 < 0 \Longrightarrow c_3 > \frac{e_1 b_1(1-n)}{c_1+1-n}$ if $a_1 > 1$ and $c_2 > \frac{a_2}{a_3}$ and $c_3 > \frac{e_1 b_1(1-n)}{c_1+1-n}$ then $\lambda_i < 0 \Rightarrow E_1$ is LAS where $i = 1, 2, 3$.

Around $E_2\left(\frac{1}{a_1}, 0, 0\right)$:

$$J_2 = \begin{pmatrix} 1 - \frac{1}{a_1} & -\frac{a_2}{a_1 a_3} & -\frac{b_1(1-n)}{a_1\left(c_1 + \frac{1-n}{a_1}\right)} \\ 0 & \frac{a_2}{a_1 a_3} - c_2 & 0 \\ 0 & 0 & \frac{e_1 b_1(1-n)}{a_1 c_1 + 1 - n} - c_3 \end{pmatrix},$$

and the eigenvalues are $\lambda_1 = 1 - \frac{1}{a_1}$, $\lambda_2 = \frac{a_2}{a_1 a_3} - c_2$, $\lambda_3 = \frac{e_1 b_1 (1-n)}{a_1 c_1 + 1 - n} - c_3$, $\lambda_1 < 1$ if $a_1 < 1$, $\lambda_2 < 0$ if $c_2 > \frac{a_2}{a_1 a_3}$, $\lambda_3 < 0$ if $c_3 > \frac{e_1 b_1 (1-n)}{a_1 c_1 + 1 - n}$.

E_2 is LAS if $a_1 < 1$ and $c_2 > \frac{a_2}{a_1 a_3}$ and $c_3 > \frac{e_1 b_1 (1-n)}{a_1 c_1 + 1 - n}$.

Since $E_2\left(\frac{1}{a_1}, 0, 0\right)$ and $a_1 < 1$, E_2 can be written as $E_2(M, 0, 0)$ where $M > 1$, so even though this equilibrium point is mathematically stable, and make sense it doesn't make sense from a biological point of view and thus we will not analyze it any further.

Around $E_4\left(\frac{c_1 c_3}{(b_1 e_1 - c_3)(1-n)}, 0, \left((n-1)^2 (b_1 e_1 - c_3)^2 + c_1 c_3 (n-1)(a_1 + 1)(b_1 e_1 - c_3) + a_1 c_1^2 c_3^2\right) \times \right.$
$\left. \times \frac{e_1 c_1}{(b_1 e_1 - c_3)^3 (n-1)^3}\right)$:

$$J_4 = \begin{pmatrix} A_{1,1} & A_{1,2} & A_{1,3} \\ A_{2,1} & A_{2,2} & A_{2,3} \\ A_{3,1} & A_{3,2} & A_{3,3} \end{pmatrix},$$

$$A_{1,1} = -\frac{c_3}{b_1 e_1 (b_1 e_1 - c_3)^2 (n-1)^2} \left((n-1)^2 (b_1 e_1 - c_3)^2 + \right.$$
$$\left. + a_1 c_1^2 c_3 (2 b_1 e_1 + c_3) + c_1 (n-1)(a_1 + 1)\left(e_1^2 b_1^2 - c_3^2\right)\right),$$
$$A_{1,2} = a_2 c_1 \frac{c_3}{(b_1 e_1 - c_3)(n-1) a_3} < 0, \quad A_{1,3} = -\frac{c_3}{e_1} < 0,$$
$$A_{2,2} = \frac{1}{a_3 (b_1 e_1 - c_3)^3 (n-1)^3} \left(c_2 a_3 (n-1)^3 (c_3 - e_1 b_1)^3 + c_1 (n-1)^2 (c_3 - e_1 b_1)^2 (-b_2 a_3 e_1 - a_2 c_3) + \right.$$
$$\left. + c_1^2 b_2 a_3 e_1 c_3 (n-1)(a_1 + 1)(c_3 - e_1 b_1) - b_2 a_3 e_1 c_3^2 a_1 c_1^3\right),$$
$$A_{3,1} = -\frac{a_1 c_1 c_3 + (b_1 e_1 - c_3)(n-1)}{(n-1)^2 (b_1 e_1 - c_3) b_1} (c_1 c_3 + (b_1 e_1 - c_3)(n-1)) > 0$$

according to the feasibility conditions.

$$A_{3,2} = \frac{b_2 e_1 c_1 e_2}{(-1+n)^3 (b_1 e_1 - c_3)^3} (c_1 c_3 + (b_1 e_1 - c_3)(n-1))(a_1 c_1 c_3 + (b_1 e_1 - c_3)(n-1)) > 0$$

according to the feasibility conditions.

$$A_{2,1} = A_{2,3} = A_{3,3} = 0.$$

And the characteristic equation is

$$\lambda^3 + L_2 \lambda^2 + L_1 \lambda + L_0 = 0,$$
$$L_2 = -(A_{1,1} + A_{2,2}), \quad L_1 = A_{1,1} A_{2,2} - A_{1,3} A_{3,1}, \quad L_0 = A_{1,3} A_{3,1} A_{2,2}.$$

According to the Routh Hurwitz Stability Criteria E_4 is LAS if L_2, $L_0 > 0$ and $L_1 L_2 > L_0$.

If $L_2 > 0$, then

$$A_{1,1} + A_{2,2} < 0. \qquad (\eta_1)$$

If $L_0 > 0$, then $A_{1,3} A_{3,1} A_{2,2} > 0$, $A_{1,3} < 0$ and $A_{3,1} > 0$ then $A_{2,2} < 0 \Rightarrow$

$$c_2 a_3 (n-1)^3 (c_3 - e_1 b_1)^3 + c_1^2 b_2 a_3 e_1 c_3 (n-1)(a_1 + 1)(c_3 - e_1 b_1) > $$
$$> c_1 (n-1)^2 (c_3 - e_1 b_1)^2 (b_2 a_3 e_1 + a_2 c_3) + b_2 a_3 e_1 c_3^2 a_1 c_1^3. \qquad (\eta_2)$$

If $L_1L_2 > L_0$, then

$$-A_{1,1}A_{2,2}(A_{1,1} + A_{2,2}) + A_{1,3}A_{3,1}A_{1,1} > 0. \qquad (\eta_3)$$

E_4 is LAS with the conditions (η_1), (η_2), (η_3).

Around $E_5\,(s^*,\, i^*,\, 0)$:

$$J_5 = \begin{pmatrix} B_{1,1} & B_{1,2} & B_{1,3} \\ B_{2,1} & B_{2,2} & B_{2,3} \\ B_{3,1} & B_{3,2} & B_{3,3} \end{pmatrix},$$

$$B_{1,1} = -3a_1 s^{*2} + (1 + 2a_1)s^* - \frac{a_2 i^*}{a_3 + i^*}, \quad B_{1,2} = -\frac{a_2 s^*}{a_3 + i^*} + \frac{a_2 s^* i^*}{\left(a_3 + i^*\right)^2} < 0,$$

$$B_{1,3} = -\frac{b_1(1-n)s^*}{c_1 + (1-n)s^*} < 0, \quad B_{2,1} = \frac{a_2 i^*}{a_3 + i^*} > 0, \quad B_{2,2} = \frac{a_2 s^*}{a_3 + i^*} - \frac{a_2 s^* i^*}{\left(a_3 + i^*\right)^2} - c_2,$$

$$B_{2,3} = -b_2 i^* < 0, \quad B_{3,1} = 0, \quad B_{3,2} = 0, \quad B_{3,3} = \frac{e_1 b_1 (1-n)s^*}{c_1 + (1-n)s^*} + e_2 b_2 i^* - c_3,$$

$$L_2 = -(B_{1,1} + B_{2,2} + B_{3,3}), \quad L_1 = B_{1,1}B_{2,2} + B_{1,1}B_{3,3} + B_{2,2}B_{3,3} - B_{1,2}B_{2,1},$$

$$L_0 = B_{1,2}B_{2,1}B_{3,3} - B_{1,1}B_{2,2}B_{3,3}.$$

According to the Routh Hurwitz Stability Criteria E_4 is LAS if L_2, $L_0 > 0$ and $L_1L_2 > L_0$.

If $L_2 > 0$, then

$$B_{1,1} + B_{2,2} + B_{3,3} < 0. \qquad (\rho_1)$$

If $L_0 > 0$, then

$$B_{1,2}B_{2,1}B_{3,3} - B_{1,1}B_{2,2}B_{3,3} > 0. \qquad (\rho_2)$$

If $L_1L_2 > L_0$, then

$$-(B_{1,1} + B_{2,2} + B_{3,3})(B_{1,1}B_{2,2} + B_{1,1}B_{3,3} + B_{2,2}B_{3,3} - B_{1,2}B_{2,1}) > B_{1,2}B_{2,1}B_{3,3} - B_{1,1}B_{2,2}B_{3,3}. \qquad (\rho_3)$$

E_5 is LAS with the conditions (ρ_1), (ρ_2), (ρ_3).

Around $\widetilde{E}(\widetilde{s},\, \widetilde{i},\, \widetilde{p})$:

$$\widetilde{J} = \begin{pmatrix} C_{1,1} & C_{1,2} & C_{1,3} \\ C_{2,1} & C_{2,2} & C_{2,3} \\ C_{3,1} & C_{3,2} & C_{3,3} \end{pmatrix},$$

$$C_{1,1} = -3a_1\widetilde{s}^{\,2} + (1 + 2a_1)\widetilde{s} - \frac{a_2\widetilde{i}}{a_3 + \widetilde{i}} - \frac{b_1(1-n)\widetilde{p}}{c_1 + (1-n)\widetilde{s}} + \frac{b_1(1-n)^2\widetilde{s}\,\widetilde{p}}{(c_1 + (1-n)\widetilde{s})^2},$$

$$C_{1,2} = -\frac{a_2\widetilde{s}}{a_3 + i^*} + \frac{a_2\widetilde{s}\,\widetilde{i}}{(a_3 + \widetilde{i})^2} < 0, \quad C_{1,3} = -\frac{b_1(1-n)\widetilde{s}}{c_1 + (1-n)\widetilde{s}} < 0, \quad C_{2,1} = \frac{a_2\widetilde{i}}{a_3 + \widetilde{i}} > 0,$$

$$C_{2,2} = \frac{a_2\widetilde{s}}{a_3 + \widetilde{i}} - \frac{a_2\widetilde{s}\,\widetilde{i}}{(a_3 + \widetilde{i})^2} - b_2\widetilde{p} - c_2, \quad C_{2,3} = -b_2\widetilde{i} < 0, \quad C_{3,1} = \frac{e_1 b_1(1-n)\widetilde{p}}{c_1 + (1-n)\widetilde{s}}\left(1 - \frac{(1-n)\widetilde{s}}{c_1 + (1-n)\widetilde{s}}\right) > 0,$$

$$C_{3,2} = e_2 b_2 \widetilde{p} > 0, \quad C_{3,3} = \frac{e_1 b_1(1-n)\widetilde{s}}{c_1 + (1-n)\widetilde{s}} + e_2 b_2 \widetilde{i} - c_3,$$

$$L_2 = -(C_{1,1} + C_{2,2} + C_{3,3}), \quad L_1 = C_{1,1}C_{2,2} + C_{1,1}C_{3,3} + C_{2,2}C_{3,3} - C_{1,2}C_{2,1} - C_{2,3}C_{3,2} - C_{1,3}C_{3,1},$$

$$L_0 = C_{1,3}C_{3,1}C_{2,2} + C_{1,2}C_{2,1}C_{3,3} + C_{1,1}C_{2,3}C_{3,2} - C_{1,3}C_{2,1}C_{3,2} - C_{1,1}C_{2,2}C_{3,3} - C_{1,2}C_{3,1}C_{2,3}.$$

According to Routh Hurwitz Stability Criteria $\widetilde{E}$ is LAS if L_2, $L_0 > 0$ and $L_1 L_2 > L_0$.

The stability outcomes align with observations in real-world systems, such as the role of *Toxoplasma gondii* in modulating prey – predator dynamics. These parallels between theory and ecological evidence underscore the applicability of our models in understanding and predicting complex interactions in natural ecosystems.

7. Extinction scenarios of the model A

In this section we shall build the conditions under which the predator and prey extinction will occur in the long term.

Take $\overline{s} = \lim\limits_{t\to\infty} \sup s(t)$, $\underline{s} = \lim\limits_{t\to\infty} \inf s(t)$, $\overline{i} = \lim\limits_{t\to\infty} \sup i(t)$, $\underline{i} = \lim\limits_{t\to\infty} \inf i(t)$, $\overline{p} = \lim\limits_{t\to\infty} \sup p(t)$, $\underline{p} = \lim\limits_{t\to\infty} \inf p(t)$ and from earlier we have $\overline{s}(t) \leqslant 1$ and let's say $\overline{i}(t) \leqslant M$ as we have proven that all the solutions are uniformly bounded.

Theorem 3. *If* $\overline{s} < \frac{1}{a_1}$ *then* $\lim\limits_{t\to\infty} s(t) = 0$.

Proof. Suppose it is not true $s(t) = \mu \neq 0$.

Choose ε s.t. $0 < \varepsilon < \frac{1}{a_1} - \overline{s}$. Then $\exists T_1 > 0$ s.t. $s(t) < \mu + \varepsilon$, $\forall t > T_1$.

Also, by definition we have for $\varepsilon > 0$ $\exists T_2 > 0$ s.t. $s(t) < \overline{s} + \varepsilon$, $\forall t > T_2$. $\forall t > \max\{T_1, T_2\}$:

$$s(t) = s(0)e^{\int\limits_0^t \left(s(1-s)(a_1 s-1) - \frac{a_2 si}{a_3+i} - \frac{b_1(1-n)sp}{c_1+(1-n)s}\right)dx} < s(0)e^{\int\limits_0^t s(1-s)(a_1 s-1)\,dx} \leqslant s(0)e^{\int\limits_0^t (1-s)(a_1 s-1)\,dx} <$$

$$< s(0)e^{\int\limits_0^t a_1\left(\overline{s}+\varepsilon-\frac{1}{a_1}\right)dx} \to 0.$$

So, as $t \to \infty$ $s(t) \to 0$; which is a contradiction.

We can conclude that even if we ignore the predation and the disease spread, the Allee effect is enough to drive the prey to extinction in the system. □

Theorem 4. *If* $\underline{i} > \dfrac{2a_3\left(1-\frac{1}{a_1}\right)}{\frac{a_2}{a_1} - 2\left(1-\frac{1}{a_1}\right)}$ *then* $\lim\limits_{t\to\infty} s(t) = 0$.

Proof. Suppose it is not true that $s(t) = \mu \neq 0$.

Choose ε s.t. $0 < \varepsilon < 1 - \frac{1}{a_1}$. Then $\exists T_1 > 0$ s.t. $s(t) < 1 + \varepsilon$, $\forall t > T_1$.

Also, by definition we have for

$$0 < \delta < \underline{i} - \frac{2a_3\left(1-\frac{1}{a_1}\right)}{\frac{a_2}{a_1} - 2\left(1-\frac{1}{a_1}\right)} \ \exists T_2 > 0 \text{ s.t. } i(t) > \underline{i} - \delta, \ \forall t > T_2.$$

$\forall t > \max\{T_1, T_2\}$:

$$s(t) = s(0)e^{\int\limits_0^t \left(s(1-s)(a_1 s-1) - \frac{a_2 si}{a_3+i} - \frac{b_1(1-n)sp}{c_1+(1-n)s}\right)dx} < s(0)e^{\int\limits_0^t s\left((a_1 s-1) - \frac{a_2 i}{a_3+i}\right)dx} < s(0)e^{\int\limits_0^t s\left(2a_1\left(1-\frac{1}{a_1}\right) - \frac{a_2(\underline{i}-\delta)}{a_3+(\underline{i}-\delta)}\right)dx} \to 0.$$

So, as $t \to \infty$ $s(t) \to 0$; which is a contradiction.

We conclude that when the Allee effect is very strong ($a_1 \approx 1$) the suspectable prey is likely to face extinction due to the slightest spread of infection. We also notice that when the disease spread in the prey population reaches a very high rate the susceptible prey is driven to extinction. □

Theorem 5. *If* $\underline{p} > \frac{2c_1(a_1-1)}{b_1(1-n)} + \frac{\frac{4a_1^2+2}{a_1}-6}{b_1}$ *then* $\lim\limits_{t\to\infty} s(t) = 0.$

Proof. Suppose it is not true that $s(t) = \mu \neq 0$.
Choose ε s.t. $0 < \varepsilon < 1 - \frac{1}{a_1}$. Then $\exists T_1 > 0$ s.t. $s(t) < 1 + \varepsilon$, $\forall t > T_1$.
Also, by definition we have for

$$0 < \delta < \underline{p} - \left(\frac{2c_1(a_1-1)}{b_1(1-n)} + \frac{\frac{4a_1^2+2}{a_1}-6}{b_1}\right) \exists T_2 > 0 \text{ s.t. } p(t) > \underline{p} - \delta,\ \forall t > T_2.$$

$\forall t > \max\{T_1, T_2\}$:

$$s(t) = s(0)e^{\int_0^t \left(s(1-s)(a_1 s-1) - \frac{a_2 si}{a_3+i} - \frac{b_1(1-n)sp}{c_1+(1-n)s}\right)dx} < s(0)e^{\int_0^t s\left((a_1 s-1) - \frac{b_1(1-n)sp}{c_1+(1-n)s}\right)dx} <$$

$$< s(0)e^{\int_0^t s\left(2a_1\left(1-\frac{1}{a_1}\right) - \frac{b_1(1-n)(\underline{p}-\delta)}{c_1+(1-n)\left(2-\frac{1}{a_1}\right)}\right)dx} < s(0)e^{\int_0^t \left(-W_1\left(\frac{W_2W_3}{b_1(1-n)} + (\underline{p}-\delta)\right)\right)dx} < 0,$$

$$W_1 = \frac{b_1(1-n)s}{c_1 + (1-n)\left(2-\frac{1}{a_1}\right)}, \quad W_2 = -2a_1\left(1-\frac{1}{a_1}\right), \quad W_3 = c_1 + (1-n)\left(2-\frac{1}{a_1}\right).$$

So, as $t \to \infty$ $s(t) \to 0$; which is a contradiction.

Our first observation is that when the Allee effect is very strong ($a_1 \approx 1$) it's very likely that the suspectable prey is going to face extinction as long as the system has a predator population (however small). Another observation is that the prey refuge effects the system ability to sustain the existence of the susceptible prey and prevent extinction. Finally, we can state that with predator getting more aggressive the suspectable is more likely to wash out of the system. □

Theorem 6. *If* $\underline{i} > \frac{a_2(1+\varepsilon)}{c_2} - a_3$ *then* $\lim\limits_{t\to\infty} i(t) = 0.$

Proof. Let $\lim\limits_{t\to\infty} i(t) = \mu \neq 0$.
For a really small ε, $\exists T_1 > 0$ s.t. $s(t) < 1 + \varepsilon$, $\forall t > T_1$.
Also, by definition we have for

$$0 < \delta < \underline{i} - \frac{a_2(1+\varepsilon)}{c_2} + a_3 \ \exists T_2 > 0 \text{ s.t. } i(t) > \underline{i} - \delta,\ \forall t > T_2.$$

$\forall t > \max\{T_1, T_2\}$:

$$\frac{di}{dt} = \frac{a_2 si}{a_3+i} - b_2 ip - c_2 i < \left(\frac{a_2 s}{a_3+i} - c_2\right) i < \left(\frac{a_2(1+\varepsilon)}{a_3+i} - c_2\right) i < \left(\frac{a_2(1+\varepsilon)}{a_3 + (\underline{i}-\delta) - c_2}\right) i,$$

$$i(t) < i(0)e^{\int_0^t \left(\frac{a_2(1+\varepsilon)}{a_3+(\underline{i}-\delta)} - c_2\right) i\, dx} \to 0$$

as $t \to \infty$ contradiction.

We can conclude that the nonlinear incidence rate adds a level of complexity to the system; developing a new case where the infected prey faces extinction.

If we take the system without the nonlinear incidence rate the expression $\frac{di}{dt}$ is going to be written as; $\frac{di}{dt} = \omega_2 si - b_2 ip - c_2 i < (\omega_2 s - c_2)i < (\omega_2(1+\varepsilon) - c_2)i$ and it would be enough to say if $c_2 > \omega_2$ then $\lim\limits_{t\to\infty} i(t) = 0$ where $\omega_2 = \frac{\beta k}{\alpha}$ and $\varepsilon\omega_2 < c_2 - \omega_2$. □

Theorem 7. *If* $\underline{p} > \frac{a_2(1+\varepsilon)}{b_2(a_3+\underline{i})}$ *then* $\lim_{t\to\infty} i(t) = 0$.

Proof. Let $\lim_{t\to\infty} i(t) = \mu \neq 0$.

For a really small ε, $\exists T_1 > 0$ s.t. $s(t) < 1 + \varepsilon$, $\forall t > T_1$.

Also, by definition we have for $0 < \delta < \underline{p} - \frac{a_2(1+\varepsilon)}{b_2(a_3+\underline{i})}$ $\exists T_2 > 0$ s.t. $p(t) > \underline{p} - \delta$, $\forall t > T_2$.

We also have $i(t) \geqslant \underline{i}$ for any t, $\forall t > \max\{T_1, T_2\}$:

$$\frac{di}{dt} = \frac{a_2 si}{a_3 + i} - b_2 ip - c_2 i < \left(\frac{a_2 s}{a_3 + i} - b_2 p\right) i < \left(\frac{a_2(1+\varepsilon)}{a_3 + \underline{i}} - b_2 p\right) i < \left(\frac{a_2(1+\varepsilon)}{a_3 + \underline{i}} - b_2(\underline{p} - \delta)\right) i,$$

$$i(t) < i(0) e^{\int_0^t \left(\frac{a_2(1+\varepsilon)}{a_3+\underline{i}} - b_2(\underline{p}-\delta)\right) i\, dx} \to 0$$

as $t \to \infty$, a contradiction.

We can conclude that even when predation is the cause driving the infected prey to extinction, the nonlinear incidence rate still adds a level of complexity to the system.

If we take the system without the nonlinear incidence rate the expression $\frac{di}{dt}$ is going to be written as; $\frac{di}{dt} = \omega_2 si - b_2 ip - c_2 i < (\omega_2 s - b_2 p)i < (\omega_2(1+\varepsilon) - b_2(\underline{p} - \delta))i$ and it would be enough to say if $\underline{p} > \frac{\omega_2(1+\varepsilon)}{b_2}$ then $\lim_{t\to\infty} i(t) = 0$ where $0 < \delta < \underline{p} - \frac{\omega_2(1+\varepsilon)}{b_2}$ and $\varepsilon > 0$ is very small. □

Theorem 8. *If* $\bar{i} < \frac{c_3 - e_1 b_1}{e_2 b_2}$ *then* $\lim_{t\to\infty} p(t) = 0$.

Proof. Let $\lim_{t\to\infty} p(t) = \mu \neq 0$.

From the definition $0 < \delta < \bar{i} > \frac{c_3 - e_1 b_1}{e_2 b_2}$ $\exists T_1 > 0$ s.t. $i(t) < \bar{i} + \delta$, $\forall t > T_1$.

We write

$$\frac{dp}{dt} = \frac{e_1 b_1 (1-n) sp}{c_1 + (1-n)s} + e_2 b_2 ip - c_3 p = \left(\frac{e_1 b_1}{\frac{c_1}{(1-n)s} + 1} + e_2 b_2 i - c_3\right) p < (e_1 b_1 + e_2 b_2(\bar{i} + \delta) - c_3) p,$$

$$p(t) < p(0) e^{\int_0^t (e_1 b_1 + e_2 b_2(\bar{i}+\delta) - c_3) p\, dx} \to 0$$

as $t \to \infty$, a contradiction.

We can conclude that in the existence of prey refuge for susceptible prey, the infected prey plays the main role in the survival of the predator. This suggests that the infected prey is more preferable than the susceptible prey to the predator. □

8. Global stability

In this section, we shall discuss the Global stability of the local asymptotically stable points from earlier E_0, E_1, E_4 of model A.

Global stability of the equilibrium point $E_0(0, 0, 0)$

For $E_0(0, 0, 0)$ the system is globally asymptotically stable if the conditions of Theorems 3, 7, 8 or 4, 6, 7 or 5, 7, 8 or 3, 6, 8 or 4, 6, 8 or 5, 6, 8 are satisfied.

Global stability of the equilibrium point $E_1(1, 0, 0)$

To prove the stability of our equilibrium points, we will be using the Lyapunov method. The Lyapunov function that we will be using is often used in ecological models and epidemic models in the following form [Liu, Zhang, 2011]:

$$\sum_{i=1}^{n} a_i \left(x_i - x_i^* - x_i^* \ln \frac{x_i}{x_i^*} \right).$$

Adjusting to our system of equations, we form the function $L\colon \Omega \in R^3 \to R$ with:

$$L(s,\ i,\ p) = \left(s - s^* - s^* \ln \frac{s}{s^*} \right) + a_1 \left(i - i^* - i^* \ln \frac{i}{i^*} \right) + a_2 \left(p - p^* - p^* \ln \frac{p}{p^*} \right),$$

where $\forall (s,\ i,\ p) \in \Omega$ and a_1, a_2, a_3 are real numbers. The function L is a Lyapunov function because it fulfills the definition of the Lyapunov function which will be shown as follows.

The function L is continuous in Ω because it contains logarithms and has a first partial derivative that is continuous in Ω. For any $E = (s,\ i,\ p) \in \Omega$ with $\neq E^*$, then $L(t) > 0$, then if $E = E^*$ then $L(t) = 0$.

It will be shown that $L(t) > 0$ when $E \neq E^*$.

Suppose $\frac{E}{E^*} = q$ and $(q) = E - E^* - E^* \ln \frac{E}{E^*}$, then:

$$g(q) = E - E^* - E^* \ln \frac{E}{E^*},$$
$$g(q) = E^*(q - 1 - \ln q).$$

Note that point $q = 1$ is the minimum point of $g(q)$ where $g(1) = 0$, because $g'(1) = 0$ and $g''(q) = \frac{1}{q^2} > 0$. Thus, we get $g(q) = E - E^* - E^* \ln \frac{E}{E^*} > 0$, for $E \neq E^*$.

Now we modify the Lyapunov function to apply on E_1, so we take

$$L_1(s,\ i,\ p) = (s - 1 - \ln s) + i + p.$$

L_1 is obviously positive definite and continuous on

$$\Pi_1 = \left\{ (s,\ i,\ p) \in R_+^3 \colon s > \frac{1}{a_1},\ a_1 > 1,\ c_2 > \frac{a_2}{a_3},\ c_3 > \frac{e_1 b_1 (1-n)}{c_1 + 1 - n} \right\}.$$

Furthermore,

$$\frac{dL_1}{dt} = \frac{s-1}{s} \left(s(1-s)(a_1 s - 1) - \frac{a_2 si}{a_3 + i} - \frac{b_1(1-n)sp}{c_1 + (1-n)s} \right) +$$
$$+ \frac{a_2 si}{a_3 + i} - b_2 ip - c_2 i + \frac{e_1 b_1 (1-n) sp}{c_1 + (1-n)s} + e_2 b_2 ip - c_3 p = -(1-s)^2 (a_1 s - 1) + \left(\frac{a_2}{a_3 + i} - c_2 \right) i +$$
$$+ \frac{b_1(1-n)p}{c_1 + (1-n)s} (e_1 - 1) + b_2 ip(e_2 - 1) + \left(\frac{b_1(1-n)p}{c_1 + (1-n)s} - c_3 \right) p$$

in Π_1 we have $s > \frac{1}{a_1}$ and from the local stability conditions we have $c_2 > \frac{a_2}{a_3}$ and $c_3 > \frac{e_1 b_1 (1-n)}{c_1 + 1 - n}$.

We get $\frac{dL_1}{dt} < 0$.

Also, $L_1(1, 0, 0) = 0$ as the only solution of model (7) that satisfies $s = 1$ is the equilibrium, LaSalle Theorem [Cui, Du, Wang, 2020] implies GAS.

Global stability of the equilibrium point $E_4(\overline{s}, 0, \overline{p})$

Now we modify the Lyapunov function to apply on $E_4(\overline{s}, 0, \overline{p})$, so we take

$$L_4(s, i, p) = A\left(\overline{s} - s + \overline{s}\ln\frac{s}{\overline{s}}\right) + i + B\left(p - \overline{p} - \overline{p}\ln\frac{p}{\overline{p}}\right), \quad A > 0.$$

L_4 is obviously positive definite and continuous on

$$\Pi_4 = \left\{(s, i, p) \in R_+^3 : 0 < s < \frac{1}{a_1} < \frac{c_1c_3}{(b_1e_1 - c_3)(1-n)} < 1, \right.$$
$$\frac{e_1c_1(a_1c_1c_3 + (b_1e_1 - c_3)(n-1))(c_1c_3 + (b_1e_1 - c_3)(n-1))}{(b_1e_1 - c_3)^3(n-1)^3} < p < 1,$$
$$\left. c_2 > \frac{a_2}{a_3} > \frac{a_2c_1c_3}{a_3(b_1e_1 - c_3)(1-n)}\right\}.$$

Furthermore,

$$\frac{dL_4}{dt} = A\left(\frac{\overline{s}}{s} - 1\right)\left(s(1-s)(a_1s - 1) - \frac{a_2si}{a_3 + i} - \frac{b_1(1-n)sp}{c_1 + (1-n)s}\right) +$$
$$+ \frac{a_2si}{a_3 + i} - b_2ip - c_2i + B\left(1 - \frac{\overline{p}}{p}\right)\left(\frac{e_1b_1(1-n)sp}{c_1 + (1-n)s} + e_2b_2ip - c_3p\right) = A(\overline{s} - s)(1-s)(a_1s - 1) -$$
$$- A(\overline{s} - s)\frac{a_2i}{a_3 + i} - A\frac{b_1(1-n)p}{c_1 + (1-n)s}(\overline{s} - s) + \frac{a_2si}{a_3 + i} - c_2i + b_2i(B(p - \overline{p})e_2 - p) +$$
$$+ B(p - \overline{p})\left(\frac{(e_1b_1 - c_3)(1-n)s - c_3c_1}{c_1 + (1-n)s} - \frac{c_3(1-n)s}{c_1 + (1-n)s}\right) < A(\overline{s} - s)(1-s)(a_1s - 1) -$$
$$-A(\overline{s} - s)\frac{a_2i}{a_3 + i} - A\frac{b_1(1-n)p}{c_1 + (1-n)s}(\overline{s} - s) + \left(\frac{a_2}{a_3} - c_2\right)i + b_2i(B(p - \overline{p})e_2 - p) + B(p - \overline{p})\frac{\frac{(e_1b_1 - c_3)(1-n) - a_1c_3c_1}{a_1}}{c_1 + (1-n)s}.$$

Set $A > 0$ and $0 < B < 1$.

In Π_4 we have $p > \overline{p}$, $s < \frac{1}{a_1} < \overline{s}$ and $c_2 > \frac{a_2}{a_3}$.

From the feasibility conditions of E_4 we have $a_1c_3c_1 > (e_1b_1 - c_3)(1-n)$.

We get $\frac{dL_4}{dt} < 0$.

Also, $L_4(\overline{s}, 0, \overline{p}) = 0$ as the only solution of model (5) that satisfies $s = \overline{s}$, $p = \overline{p}$ and $i = 0$ is the equilibrium, LaSalle Theorem implies GAS.

9. Bifurcation analysis

In this section we explored bifurcations that might occur in system (5) using Sotomayor's Theorem [Mondal, Samanta, 2020].

Theorem 9. *System* (5) *undergoes a transcritical bifurcation with respect to the bifurcation parameter* C_3 *around* $E_1(1, 0, 0)$ *if,* $c_3 = \frac{e_1b_1(1-n)}{c_1 + 1 - n} = c_{3[TC_1]}$ *keeping the following condition,* $c_2 > \frac{a_2}{a_3}$ *and* $a_1 > 1$.

Proof. For $E_1(1, 0, 0)$ we have the following eigenvalues: $\lambda_1 = 1 - a_1$, $\lambda_2 = \frac{a_2}{a_3} - c_2$, $\lambda_3 = \frac{e_1 b_1(1-n)}{c_1+1-n} - c_3$,

$$J_1 = \begin{pmatrix} 1 - a_1 & -\frac{a_2}{a_3} & -\frac{b_1(1-n)}{c_1+1-n} \\ 0 & \frac{a_2}{a_3} - c_2 & 0 \\ 0 & 0 & \frac{e_1 b_1(1-n)}{c_1+1-n} - c_3 \end{pmatrix}.$$

If we take $c_3 = \frac{e_1 b_1(1-n)}{c_1+1-n}$ the eigenvalues can be written as $\lambda_1 = 1 - a_1$, $\lambda_2 = \frac{a_2}{a_3} - c_2$, $\lambda_3 = 0$ and the Jacobean matrix can be written as

$$J_1 = \begin{pmatrix} 1 - a_1 & -\frac{a_2}{a_3} & -\frac{b_1(1-n)}{c_1+1-n} \\ 0 & \frac{a_2}{a_3} - c_2 & 0 \\ 0 & 0 & 0 \end{pmatrix}.$$

Now the eigenvector corresponding to $\lambda = 0$ for J_1; $\lambda * V = J * V$,

$$V = \left(1, 0, \frac{(1 - a_1)(c_1 + 1 - n)}{b_1(1 - n)}\right)^T$$

the eigenvector corresponding to $\lambda = 0$ for J_1^T; $\lambda * U = J^T * U$, $U = (0, 0, 1)^T$ and then we can write

$$\Omega_1 = W^T * f_{c_3}\left(E_1, C_{3[TC_1]}\right) = 0,$$

$$\Omega_2 = W^T * \left[Df_{c_3}\left(E_1, C_{3[TC_1]}\right)V\right] = -\frac{(1 - a_1)(c_1 + 1 - n)}{b_1(1 - n)} \neq 0,$$

$$\Omega_3 = W^T * \left[Df_{c_3}\left(E_1, C_{3[TC_1]}\right)(V, V)\right] = \frac{2c_1 e_1(1 - a_1)}{c_1 + (1 - n)} \neq 0.$$

According to Sotomayor's theory there is a transactional bifurcation at $E_1(1, 0, 0)$ for $C_3 = C_{3[TC_1]}$. □

10. Numerical simulation and discussion

We conducted numerical simulations to verify our analytic theoretical findings using the fourth-order Runge – Kutta subjected to the positive initial conditions $s(0) = s_0$, $i(0) = i_0$, $p(0) = p_0$ using MATLAB R2022a. we carried out the numerical simulations with an assumed set of parameters to test the effect of certain factors such as the Allee effect, prey refuge, predation rates, etc.

$GP = \{a_1 = 1.2, a_2 = 0.02, a_3 = 0.002, b_1 = 1.1, b_2 = 500, c_1 = 0.1, c_2 = 11, c_3 = 0.4, e_1 = 0.35, e_2 = 0.5, n = 0.5\}$, with the initial conditions $IC_0 = \{s_0 = 0.65, i_0 = 0.4, p_0 = 0.2\}$, and then varying some of the parameters' value according to the feasibility, LAS and GAS conditions of each feasible equilibrium point we have.

The simulations in (Fig. 1) confirms our theoretical findings, showing that the trajectories of the system are globally asymptotically stable at E_0. We used the same parametric values as in GP along with the initial values IC_0. The graph visually demonstrates how the system's trajectories approach the equilibrium point, providing further evidence for the stability of E_0 in the eco-epidemiological model. It can also be observed from comparing Fig. 1, *a* and Fig. 1, *b* that the prey refuge slows the extinction as it reduces the interaction between the predator and the prey. In Fig. 1, *c* it is seen that the equilibrium point E_0 becomes unfeasible and the solutions approaches the stable equilibrium point $E_1(1, 0, 0)$ [Gaber, Herdiana, Widowati, 2024].

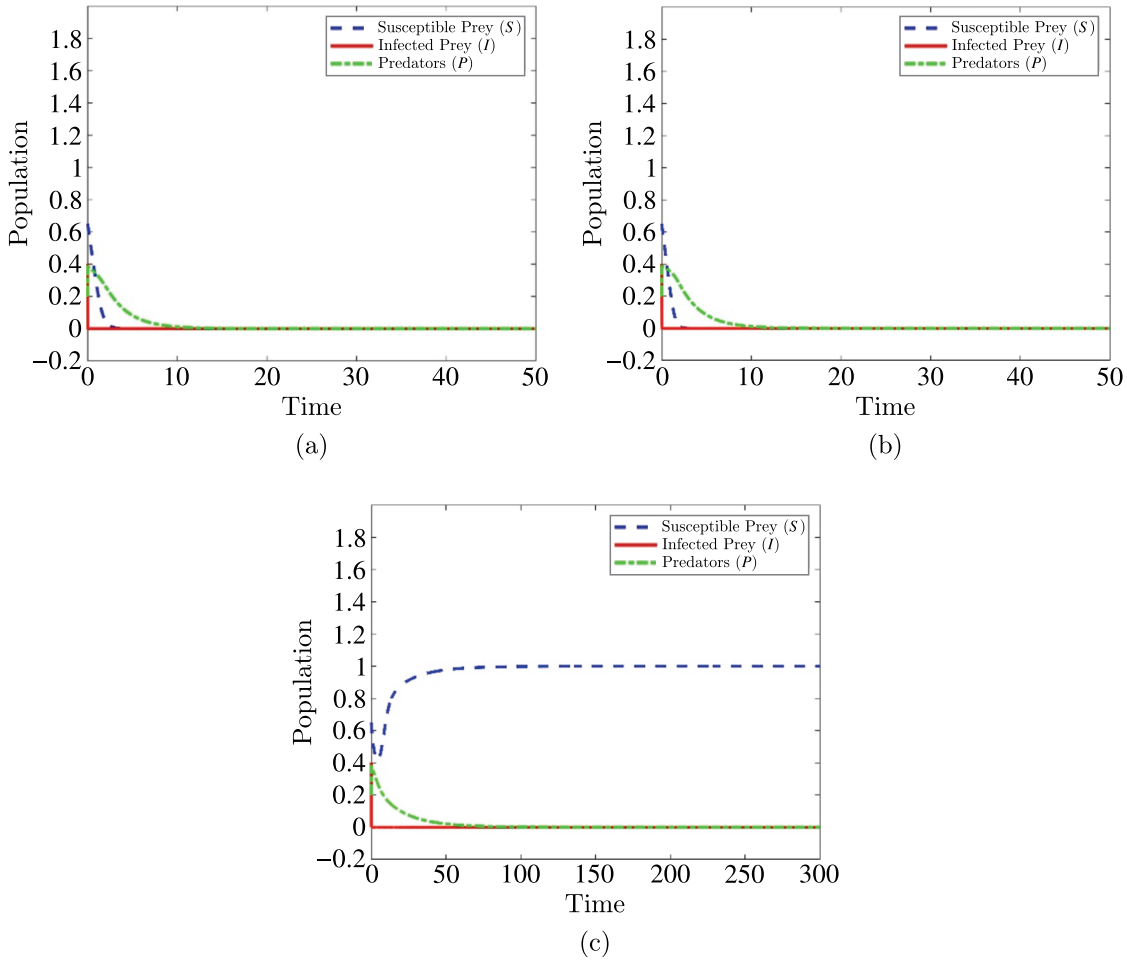

Figure 1. MATLAB simulation for globally stable behavior of E_0. The graph depicts the trajectories of a system approaching the stable equilibrium point. The x-axis represents time, while the y-axis represents the values of the system. (a) with refuge and Allee effect, (b) without prey refuge, (c) without prey refuge nor the Allee effect

The MATLAB simulation presented in (Fig. 2) demonstrates the globally stable behavior of equilibrium point $E_1(1, 0, 0)$, confirming our theoretical findings. We obtain E_1 by raising the value of a_1 to 3.4, keeping the other values in GP the same. The graph showcases four distinct scenarios (a, b, c, and d).

In Fig. 2, *a*, both the refuge and Allee effect are considered, the trajectories of the system approach the stable equilibrium point $E_1(1, 0, 0)$. This indicates that the presence of prey refuge and the Allee effect contribute to the system's stability.

In Fig. 2, *b*, the absence of prey refuge leads to the washout of all three species from the system. Consequently, the trajectories approach the stable equilibrium point E_0. This highlights the significance of prey refuge in maintaining the population dynamics and preventing extinction.

Figure 2, *c* explores the impact of eliminating or reducing the prey refuge while increasing the value of parameter a_1 to 3.8. The trajectories in this scenario approach the stable equilibrium point $E_1(1, 0, 0)$, suggesting that lowering the Allee effect threshold becomes crucial in preventing extinction when prey refuge is eliminated or reduced.

Finally, Fig. 2, *d* investigates the system's behavior without both prey refuge and the Allee effect. As previously suggested by [Gaber, Herdiana, Widowati, 2024], the trajectories in this case also converge towards the stable equilibrium point $E_1(1, 0, 0)$.

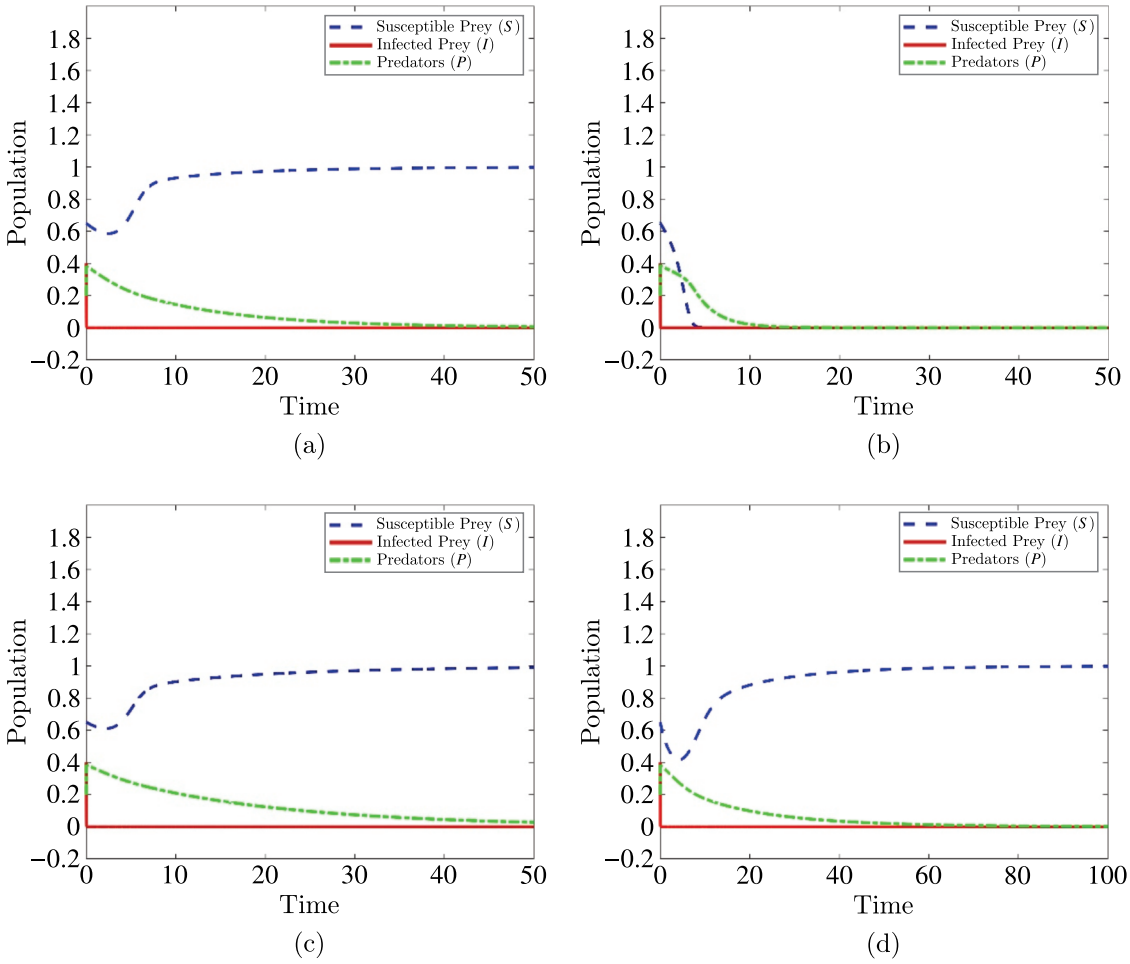

Figure 2. MATLAB simulation for Globally stable behavior of E_1. The graph depicts the trajectories of a system approaching the stable equilibrium point $E_1(1, 0, 0)$. The x-axis represents time, while the y-axis represents the values of the system. (a) with refuge and Allee effect, (b) without prey refuge and we can notice that for the same parametric values the 3 species wash-out of the system and the trajectories approach the stable equilibrium point E_0, (c) without prey refuge raising a_1 value to 3.8, (d) without prey refuge nor the Allee effect [Gaber, Herdiana, Widowati, 2024]

The MATLAB simulation presented in (Fig. 3) demonstrates the globally stable behavior of equilibrium point E_4 confirming our theoretical findings. The parameters used in the simulation are as in GP except for $a_1 = 3.8$ and $c_3 = 0.3$. The graph showcases four distinct scenarios (a, b, c, and d).

Figure 3, *a* represents the system with both prey refuge and the Allee effect. The trajectories in this scenario approach the stable equilibrium point $E_4(\overline{s}, 0, \overline{p})$. This observation confirms the globally stable behavior of E_4 when these factors are considered.

In Fig. 3, *b*, the absence of prey refuge results in the washout of all three species from the system. The trajectories converge towards the stable equilibrium point E_0, emphasizing the crucial role of prey refuge in maintaining population dynamics and preventing extinction.

Figure 3, *c* explores the impact of eliminating or reducing the prey refuge while simultaneously decreasing parameter b_1 from 1.1 to 0.95. The trajectories in this scenario approach the stable equilibrium point $E_4(\overline{s}, 0, \overline{p})$. This suggests that, if we decrease or eliminate the prey refuge, the predation rate would need to be reduced to prevent extinction.

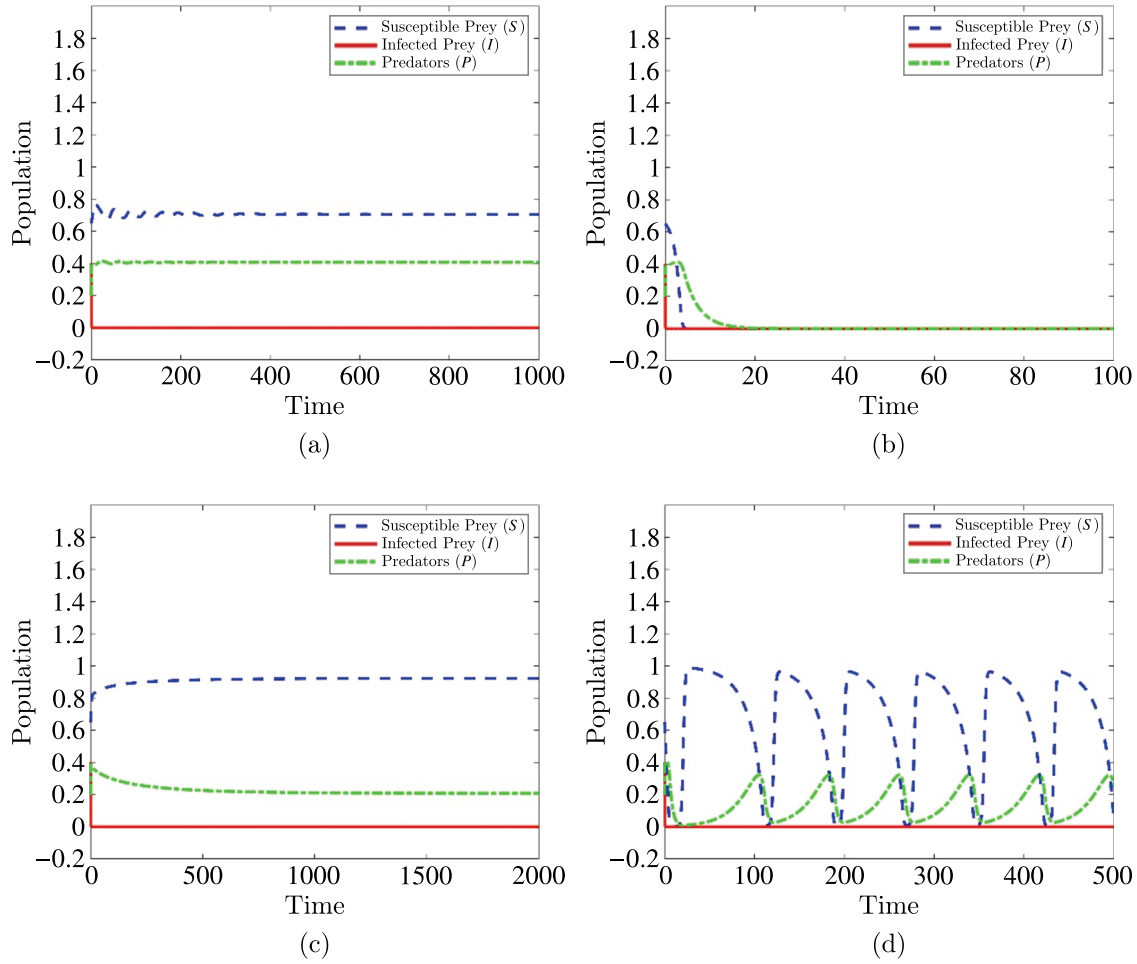

Figure 3. MATLAB simulation for Globally stable behavior of E_4. The graph depicts the trajectories of a system approaching the stable equilibrium point $E_4(\overline{s}, 0, \overline{p})$. The graph consists of four figures (a, b, c, and d) that showcase different scenarios. Figure 3, *a* represents the system with both prey refuge and the Allee effect. The trajectories in this scenario approach the stable equilibrium point $E_4(\overline{s}, 0, \overline{p})$. In Fig. 3, *b*, the absence of prey refuge results in the washout of all three species from the system. Figure 3, *c* explores the impact of eliminating or reducing the prey refuge while simultaneously decreasing parameter b_1 from 1.1 to 0.95. Lastly, Fig. 3, *d* investigates the system's behavior without both prey refuge and the Allee effect. The trajectories in this case exhibit an unstable state around $E_4(\overline{s}, 0, \overline{p})$

Lastly, Fig. 3, *d* investigates the system's behavior without both prey refuge and the Allee effect. The trajectories in this case exhibit an unstable state around $E_4(\overline{s}, 0, \overline{p})$, indicating that the absence of prey refuge and the Allee effect may lead to instability in the system.

Overall, this MATLAB simulation provides valuable insights into the significance of considering factors such as prey refuge and the Allee effect in eco-epidemiological models. The diverse scenarios presented in the graphs exemplify the importance of comprehensive analysis to ensure the stability and preservation of ecological systems.

Based on the portrait phase in (Fig. 4), we have observed an unstable limit cycle initially. This means that the system exhibits oscillations around a closed trajectory.

As time progresses, the trajectory appears to move toward the equilibrium point E_4. This behavior suggests that the system is transitioning from the unstable limit cycle toward a stable state.

The MATLAB simulation presented in (Fig. 5) demonstrates the globally stable behavior of equilibrium point $E_5(s, i, 0)$, confirming our theoretical findings. We made the following changes

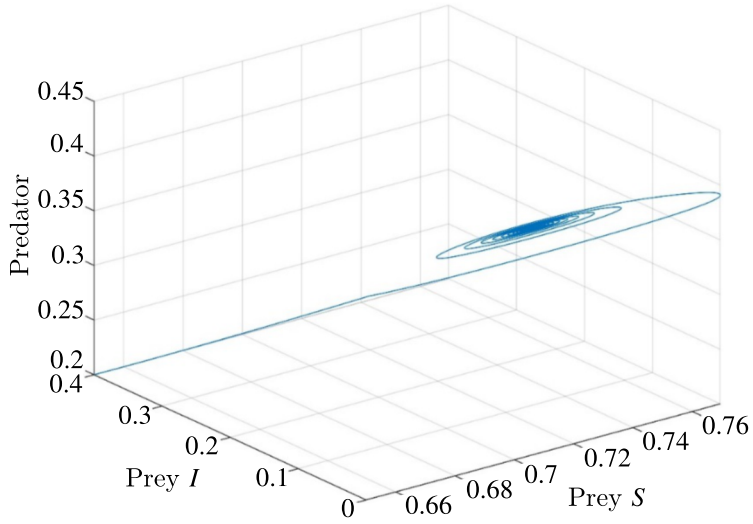

Figure 4. Dynamics Portrait Phase for the solution of the model A around E_4. This 3D plot illustrates the behavior of the studied predator – prey system. The trajectory (shown in blue) starts with an unstable limit cycle, spiraling around the equilibrium point E_4. As time progresses, the system transitions toward stability, converging toward E_4

on GP, $a_1 = 3.4$, $b_2 = 0.25$, $c_2 = 0.1$. The graph consists of three figures (a, b, c) that showcase different scenarios.

Figure 5, *a* represents the system with both prey refuge and the Allee effect. The susceptible prey population (S) remains relatively constant at around 1. Infected prey (I) stabilizes near 0.2 and the predator (P) populations washes out of the system and stabilize close to zero. With both the prey refuge and Allee effect in place, the system achieves a stable equilibrium point E_5. The higher susceptible prey population ensures better control over infected prey and predators. In Fig. 5, *b* we explore the absence of prey refuge. Susceptible prey (S) still stabilizes at around 1, but it takes more time to reach stability compared to Fig. 5, *a*. Infected prey (I) and predator (P) populations remain minimal but slightly higher than in Fig. 5, *a*. Without prey refuge, there is a slight increase in predator and infected prey populations, but the system still maintains control. Figure 5, *c* investigates the system's behavior without both prey refuge and the Allee effect. The stabilization patterns are similar to those shown in Fig. 5, *b*, but susceptible prey (S) stabilizes more quickly. It can be noticed that removing both effects leads to quicker stabilization of susceptible prey while keeping infected prey and predators at low levels.

The MATLAB simulation presented (in Fig. 6) demonstrates the globally stable behavior of equilibrium point $\widetilde{E}(\widetilde{s}, \widetilde{i}, \widetilde{p})$ confirming our theoretical findings. We made the following changes on GP, $a_1 = 3.4$, $a_2 = 0.08$, $b_2 = 1.5$, $c_1 = 0.1$, $c_2 = 0.1$. The graph consists of three figures (a, b, c) that showcase different scenarios.

Figure 6, *a* includes both prey refuge and the Allee effect. All three species stabilize at specific population levels around the equilibrium point $\widetilde{E}$. It is noticeable that Susceptible Prey (S) population stabilizes at a relatively high level. Infected Prey (I) population also stabilizes but at a lower level than susceptible prey. Predators (P) population stabilizes, maintaining the lowest population level among the three species.

Figure 6, *b* shows the absence of prey refuge. Both the susceptible prey (S) and infected prey (I) populations become extinct. Predators (P) population also goes extinct. The absence of prey refuge leads to the collapse of the entire system.

Figure 6, *c* explores the system's behavior without both prey refuge and the Allee effect. The infected prey population (I) stabilizes at a low level, similar to Fig. 6, *a*. Susceptible Prey (S) population

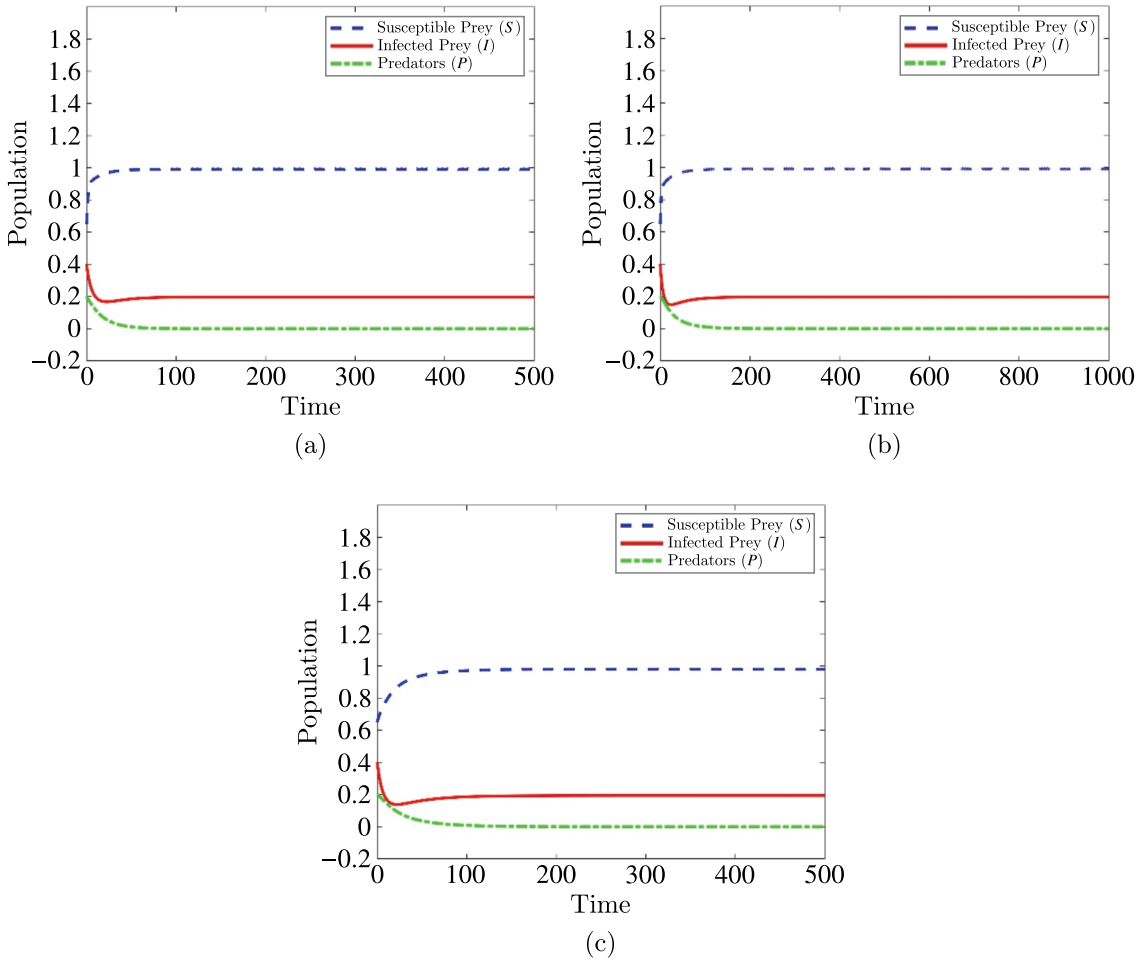

Figure 5. MATLAB simulation for Globally stable behavior of E_5. The graph depicts the trajectories of a system approaching the stable equilibrium point $E_5(s, i, 0)$. The graph consists of three figures (a, b, c) that showcase different scenarios. Figure 5, *a* represents the system with both prey refuge and the Allee effect. Figure 5, *b* shows the case of the absence of prey refuge. Figure 5, *c* explores the system's behavior without both prey refuge and the Allee effect. In the three cases the trajectories in this scenario approach the stable equilibrium point E_5

stabilizes similarly to Fig. 6, *a*. Predators (P) also stabilize, with their population level resembling that of Fig. 6, *a*.

In Fig. 7, we explore different values for the parameter a_2 around $\widetilde{E}$.

Figure 7, *a* (for $a_2 = 0.2$). This scenario corresponds to a higher infection rate relative to the growth rate of susceptible prey. The infected prey population (I) stabilizes at a low level. Susceptible Prey (S) population remains stable. Predators (P) population stabilizes, similar to Fig. 6. Figure 7, *b* (for $a_2 = 0.15$). Here, we consider a slightly lower infection rate compared to Fig. 7, *a*. Infected prey (I) population stabilizes at a slightly lower level than in Fig. 7, *a*. Susceptible Prey (S) population remains stable but at a higher level than Fig. 7, *a*. Predators (P) population stabilizes, at a lower level than Fig. 7, *a*. Figure 7, *c* (for $a_2 = 0.1$). In this case, we explore an even lower infection rate. Infected prey (I) population stabilizes at a slightly lower level than in Fig. 7, *a*. Susceptible Prey (S) population remains stable but at a higher level than Fig. 7, *a*. Predators (P) population stabilizes, at a lower level than Fig. 7, *a*. We can notice that lowering the infection rate raises the level of the susceptible prey

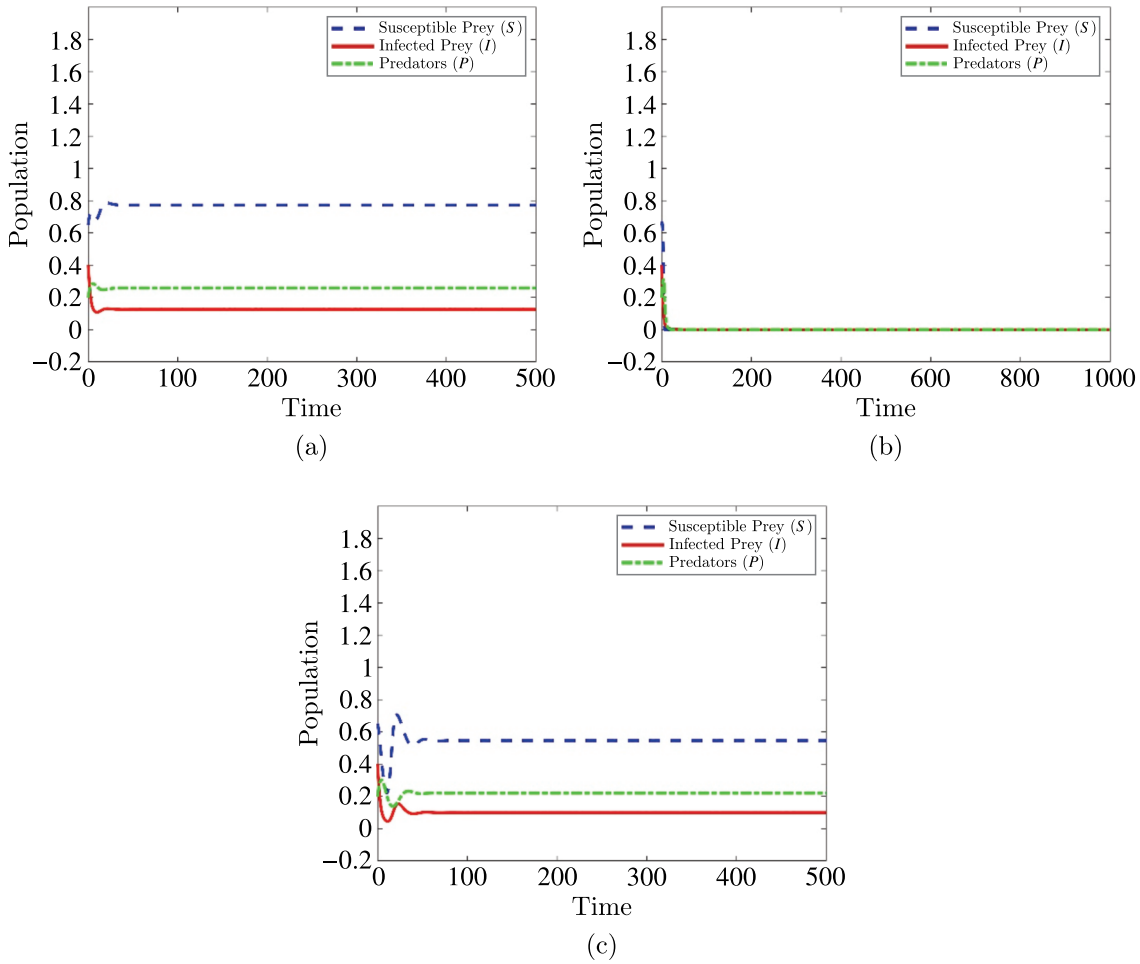

Figure 6. MATLAB simulation for Globally stable behavior of $\widetilde{E}(\widetilde{s}, \widetilde{i}, \widetilde{p})$. The graph depicts the trajectories of a system approaching the stable equilibrium point $\widetilde{E}(\widetilde{s}, \widetilde{i}, \widetilde{p})$. The graph consists of three figures (a, b, c) that showcase different scenarios. Figure 6, *a* represents the system with both prey refuge and the Allee effect. Figure 6, *b* shows the case of the absence of prey refuge. Figure 6, *c* explores the system's behavior without both prey refuge and the Allee effect

population and lower the predator population level. However, it is only slightly reducing the infected prey population rate.

The graphical representation in (Fig. 8) provides valuable insights into the dynamics of our eco-epidemiological model.

Figure 8, *a* (c_3 = 0.33): at this parameter value, both equilibrium points $E_1(1, 0, 0)$ and $E_4(\overline{s}, 0, \overline{p})$ are stable but remain separate from each other. The system exhibits a predictable behavior, with no significant changes in stability around E_1. Figure 8, *b* (c_3 = 0.320833): as we approach the bifurcation value, E_1 and E_4 collide this event is known as transcritical bifurcation. During this collision, the stability properties of the equilibrium points switch places. E_1 loses stability, while E_4 gains stability. This phenomenon confirms our theoretical predictions and highlights the critical role of parameter c_3. Figure 8, *c* (c_3 = 0.32): just below the bifurcation value, only E_4 remains stable post-collision. The system settles into a new equilibrium configuration, where E_4 dominates. Figure 8, *d* (c_3 = 0.3): further reducing c_3 maintains the newfound stability. E_4 continues to be the stable point, emphasizing the lasting impact of the bifurcation event.

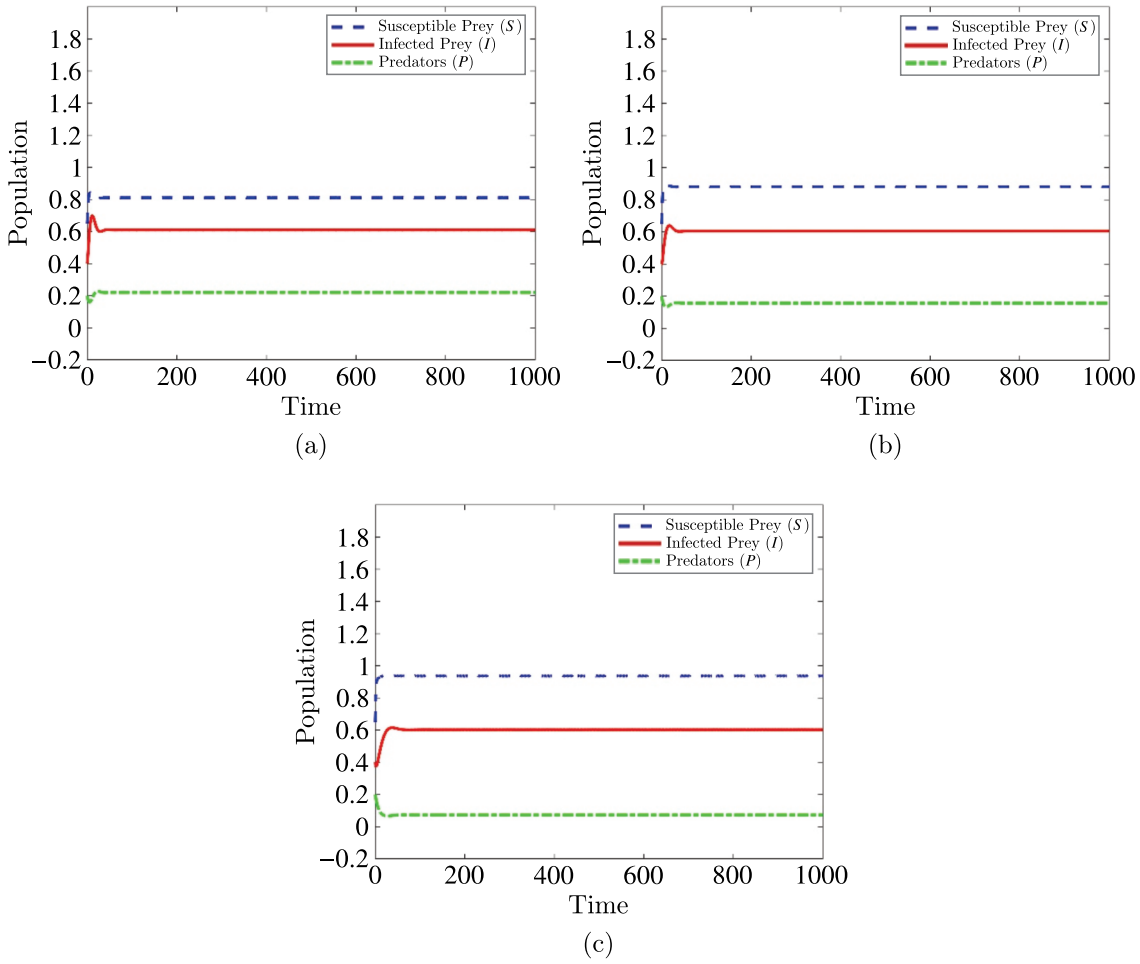

Figure 7. Study of predator – prey dynamics around $\widetilde{E}(\widetilde{s}, \widetilde{i}, \widetilde{p})$ with varying infection rate. (a) $a_2 = 0.2$; (b) $a_2 = 0.15$; (c) $a_2 = 0.1$

Figure 9 shows the solution behavior and phase portraits of an eco-epidemiological model under different parameter specifications with parameters' values of ($b_1 = 0.35$, $c_1 = 0.101123595$, $c_2 = 0.3$, $c_3 = 0.1$). Figures 9, *a* and 9, *b* depict the base model without an Allee effect or susceptible prey refuge. In this scenario, a Hopf bifurcation occurs as the parameter c_1 is varied, indicated by the limit cycle emerging in graph 9, *b*. This demonstrates that the dynamics of the system transition from a stable equilibrium to oscillations see [Gaber, Herdiana, Widowati, 2024]. Figures 9, *c* and 9, *d* examine the impact of including an Allee effect ($a_1 = 3.8$) and susceptible prey refuge ($n = 0.5$) on the model's behavior. Notably, the limit cycle disappears, and the solutions converge monotonically to a single stable equilibrium point (E_4). This implies that accounting for an Allee threshold below which population growth is slowed and the existence of a refuge that removes susceptible prey from interaction stabilizes the system. No bifurcation dynamics are present.

11. Conclusion

In this study, we developed two eco-epidemiological models to investigate population dynamics accounting for disease transmission alongside predator – prey and refuge-seeking interactions. The overarching goal was to evaluate how the inclusion of prey refuge habitat and an Allee effect might impact system stability and resilience.

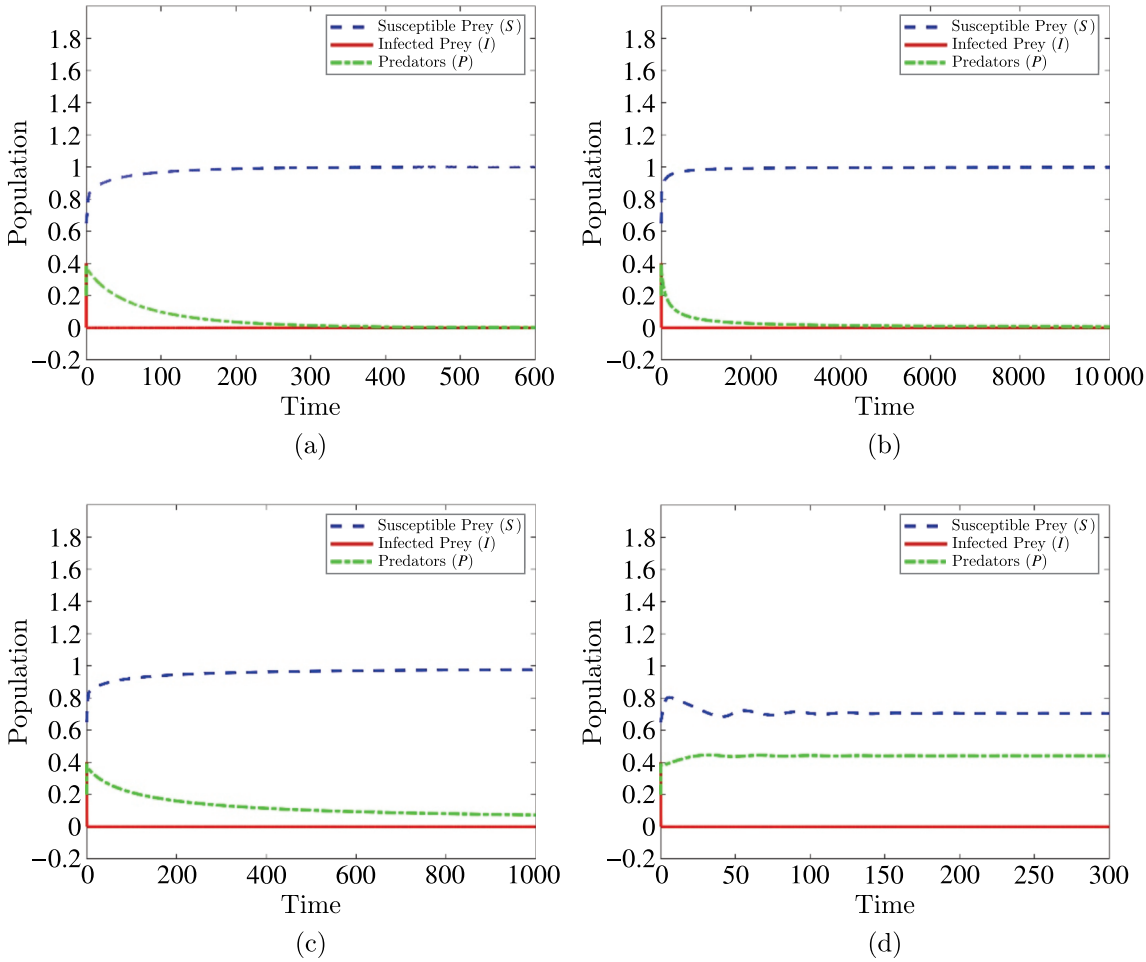

Figure 8. Dynamics of the eco-epidemiological model around equilibrium point $E_1(1, 0, 0)$. In this figure, we explore the impact of the parameter c_3 (the natural death rate of the predator divided by the growth rate of the susceptible prey) on the behavior of the system. The figure comprises four subfigures labeled a, b, c, and d, each corresponding to different values of c_3. Figure 8, *a* ($c_3 = 0.33$): at this value, the system exhibits a stable behavior around E_1. Figure 8, *b* ($c_3 = 0.320833$): here, we encounter a critical point (the bifurcation value). The equilibrium points $E_1(1, 0, 0)$ and $E_4(\overline{s}, 0, \overline{p})$ collide, leading to a significant change in stability. Figure 8, *c* ($c_3 = 0.32$): just below the bifurcation value, we observe the aftermath of the collision. E_1 loses stability, while E_4 gains stability. Figure 8, *d* ($c_3 = 0.3$): at this lower value, the new stability persists over time

Model A incorporated prey refuge availability and a predation-based Allee effect, while model B omitted these factors for comparison. Through mathematical analysis and simulation, key findings emerged regarding local and global stability properties at equilibrium states under different scenarios.

Our stability assessments revealed that model A shows a higher tendency toward extinction when the Allee effect is strong enough.

Bifurcation analyses revealed qualitative behavioral shifts triggered by parametric variations such as predator death rates or prey growth rates. Model A experienced a transcritical bifurcation that showed critical population threshold responses. Model B manifested additional bifurcation types in the absence of refuge and Allee stabilizing impacts.

Notably, disease burden and population persistence were positively influenced by refuge habitat which curbed predator – prey interactions. The Allee effect also calibrated stability through increased sensitivity to small population sizes. Our formulation successfully captured the complexity arising from disease transmission interacting with predation and density dependence.

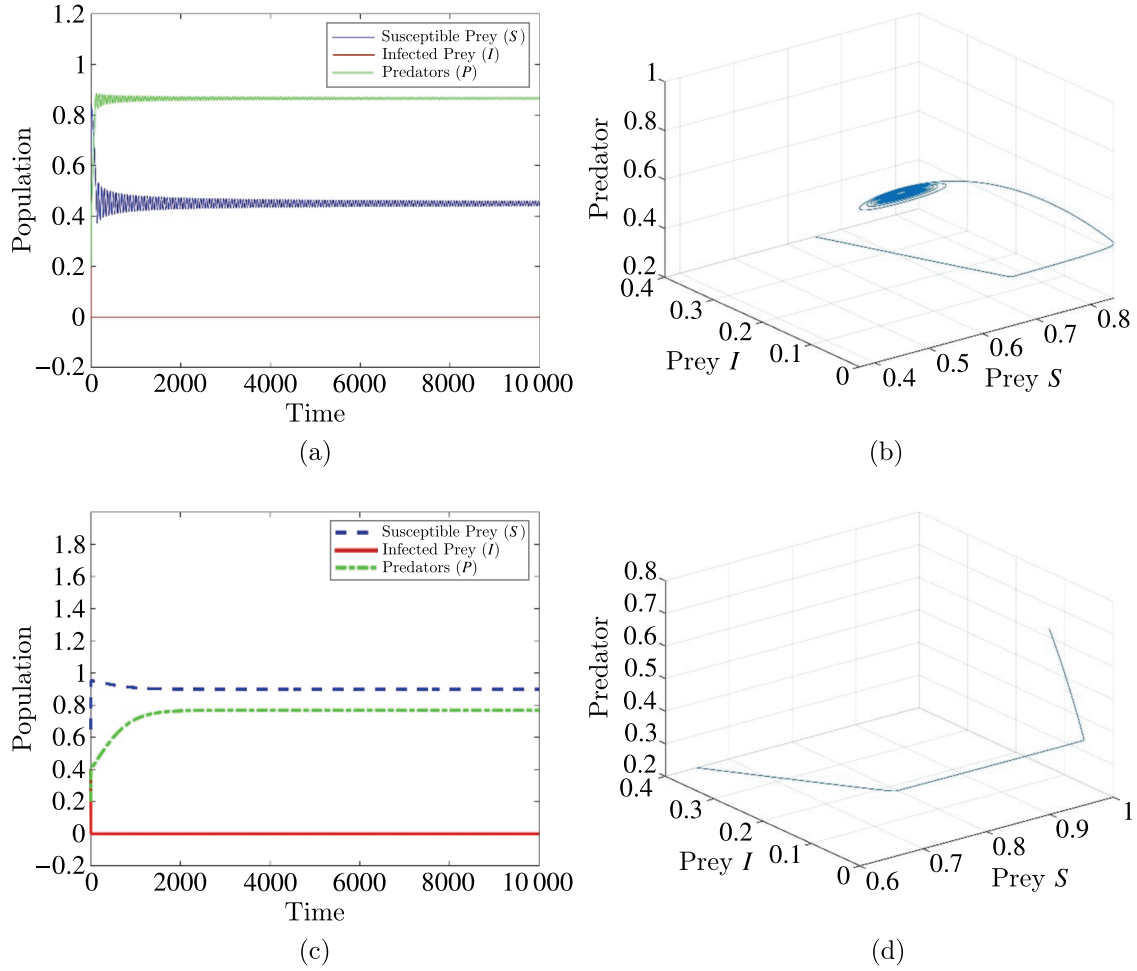

Figure 9. Comparison of solution behaviors and phase portraits for the eco-epidemiological model with and without an Allee effect and susceptible prey refuge. (a, b): model B; (c, d): model A with Allee effect ($a_1 = 3.8$) and refuge ($n = 0.5$)

The inclusion of real-world examples further supports the relevance and applicability of our models. For instance, African wild dog (*Lycaon pictus*) populations exemplify the Allee effect, where small group sizes lead to decreased hunting efficiency and lower survival rates [Courchamp, Clutton-Brock, Grenfell, 2000]. Similarly, Huffaker's mite experiments demonstrate how prey refuge habitats stabilize predator – prey dynamics [Hupfaker, 1958]. The crowding effect of infected prey is evident in avian populations affected by avian influenza (H5N1), where high densities in poultry and wild bird populations facilitate rapid disease transmission and population decline [Kilpatrick et al., 2006].

In summary, objectives to evaluate stability contributions from prey refuge and Allee effect terms, and compare system responses between models with and without these factors, were achieved. Insights gained regarding ecological tipping points enhance the understanding of managing wildlife disease spread under changing environmental conditions.

Other findings: The Allee effect can influence the stability of equilibria and potentially lead to extinction or bi-stability (two stable equilibria) depending on parameter values. The analysis identified critical thresholds for parameter values that trigger qualitative changes in the system's behavior, highlighting potential tipping points in real-world ecosystems. Model A experienced transcritical bifurcation around E_1 where E_0 and E_1 collided and exchanged stability for certain parameter values, indicating critical transitions in system behavior influenced by the death rate of the predator and the

growth rate of the susceptible prey. Model B also exhibited bifurcation phenomena, a transcritical bifurcation occurring due to the collision of E_1 and E_3 and a Hopf bifurcation around E_3 for certain parametric values. The absence of the Hopf bifurcation in model A shows the importance of prey refuge and Allee effect in stabilizing the eco-epidemiological system and avoiding ecological disasters.

References

Al-Salti N., Al-Musalhi F., Gandhi V., Al-Moqbali M., Elmojtaba I. Dynamical analysis of a prey – predator model incorporating a prey refuge with variable carrying capacity // Ecological Complexity. — 2021. — Vol. 45. — 100888. — https://doi.org/10.1016/j.ecocom.2020.100888

Anacleto M., Vidal C. Dynamics of a delayed predator – prey model with Allee effect and Holling type II functional response // Mathematical Methods in the Applied Sciences. — 2020. — Vol. 43, No. 9. — https://doi.org/10.1002/mma.6307

Anggriani N., Panigoro H. S., Rahmi E., Peter O. J., Jose S. A. A predator – prey model with additive Allee effect and intraspecific competition on predator involving Atangana – Baleanu – Caputo derivative // Results in Physics. — 2023. — Vol. 49. — 106489. — https://doi.org/10.1016/j.rinp.2023.106489

Berdoy M., Webster J. P., Macdonald D. W. Fatal attraction in rats infected with Toxoplasma gondii // Proceedings of the Royal Society of London. Series B: Biological Sciences. — 2000. — Vol. 267, No. 1452. — P. 1591–1594. — https://doi.org/10.1098/rspb.2000.1182

Cao J., Ma L., Hao P. Bifurcation analysis in a modified Leslie – Gower predator – prey model with Beddington – DeAngelis functional response // Journal of Applied Analysis & Computation. — 2023. — Vol. 13, No. 5. — P. 3026–3053.

Catenazzi A., Lehr E., Rodriguez L. O., Vredenburg V. T. Batrachochytrium dendrobatidis y el Colapso de la Riqueza de Especies y Abundancia de Anuros en el Parque Nacional del Manu, Sureste de Perú // Conservation Biology. — 2011. — Vol. 25, No. 2. — P. 382–391. — https://doi.org/10.1111/j.1523-1739.2010.01604.x

Courchamp F., Clutton-Brock T., Grenfell B. Multipack dynamics and the Allee effect in the African wild dog, *Lycaon pictus* // Animal Conservation. — 2000. — Vol. 3, No. 4. — P. 277–285. — https://doi.org/10.1111/j.1469-1795.2000.tb00113.x

Cui Q., Du Q., Wang L. Global dynamics of a generalized SIRS epidemic model with constant immigration // Mathematical Problems in Engineering. — 2020. — P. 1–9.

Flegr J. Effects of Toxoplasma on human behavior // Schizophrenia Bulletin. — 2007. — Vol. 33, No. 3. — P. 757–760. — https://doi.org/10.1093/schbul/sbl074

Gaber T., Herdiana R., Widowati. Dynamical analysis of an eco-epidemiological model experiencing the crowding effect of infected prey // Communications in Mathematical Biology and Neuroscience. — 2024. — Vol. 2024. — P. 1–28. — https://doi.org/10.28919/cmbn/8353

Han R., Dey S., Banerjee M. Spatio-temporal pattern selection in a prey – predator model with hunting cooperation and Allee effect in prey // Chaos, Solitons & Fractals. — 2023. — Vol. 171. — 113441. — https://doi.org/10.1016/j.chaos.2023.113441

Hupfaker C. B. Experimental studies on predation: dispersion factors and predator – prey oscillations. — 1958.

Kamrujjaman M., Shahriar Mahmud M., Islam M. S. Dynamics of a diffusive vaccination model with therapeutic impact and non-linear incidence in epidemiology // Journal of Biological Dynamics. — 2021. — Vol. 15 (sup1). — P. S105–S133. — https://doi.org/10.1080/17513758.2020.1849831

Kilpatrick A. M., Chmura A. A., Gibbons D. W., Fleischer R. C., Marra P. P., Daszak P. Predicting the global spread of H5N1 avian influenza // Proceedings of the National Academy of Sciences of the United States of America. — 2006. — Vol. 103, No. 51. — P. 19368–19373. — https://doi.org/10.1073/pnas.0609227103

Kumar U., Mandal P.S. Role of Allee effect on prey – predator model with component Allee effect for predator reproduction // Mathematics and Computers in Simulation. — 2022. — Vol. 193. — P. 623–665. — https://doi.org/10.1016/j.matcom.2021.10.027

Li H., Yang W., Wei M., Wang A. Dynamics in a diffusive predator – prey system with double Allee effect and modified Leslie – Gower scheme // International Journal of Biomathematics. — 2022a. — Vol. 15, No. 03. — 2250001. — https://doi.org/10.1142/S1793524522500012

Li Y.X., Liu H., Wei Y.M., Ma M., Ma G., Ma J.Y. Population dynamic study of prey – predator interactions with weak Allee effect, fear effect, and delay // Journal of Mathematics. — 2022. — 8095080. — https://doi.org/10.1155/2022/8095080

Liang Z., Meng X. Stability and Hopf bifurcation of a multiple delayed predator – prey system with fear effect, prey refuge and Crowley – Martin function // Chaos, Solitons & Fractals. — 2023. — Vol. 175. — 113955. — https://doi.org/10.1016/j.chaos.2023.113955

Liu J., Lv P., Liu B., Zhang T. Dynamics of a predator – prey model with fear effect and time delay // Complexity. — 2021. — 9184193. — https://doi.org/10.1155/2021/9184193

Liu J., Zhang T. Global stability for a tuberculosis model // Mathematical and Computer Modelling. — 2011. — Vol. 54, No. 1–2. — P. 836–845. — https://doi.org/10.1016/j.mcm.2011.03.033

Lv W., Ke Q., Li K. Dynamical analysis and control strategies of an SIVS epidemic model with imperfect vaccination on scale-free networks // Nonlinear Dynamics. — 2020. — Vol. 99, No. 2. — P. 1507–1523. — https://doi.org/10.1007/s11071-019-05371-1

Majeed S.J., Ghafel S.F. Stability analysis of a prey – predator model with prey refuge and fear of adult predator // Iraqi Journal of Science. — 2022. — Vol. 63, No. 10. — P. 4374–4387. — https://doi.org/10.24996/ijs.2022.63.10.24

Molla H., Sarwardi S., Smith S.R., Haque H. Dynamics of adding variable prey refuge and an Allee effect to a predator – prey model // Alexandria Engineering Journal. — 2022. — Vol. 61, No. 6. — P. 4175–4188. — https://doi.org/10.1016/j.aej.2021.09.039

Mondal S., Samanta G.P. Dynamics of a delayed predator – prey interaction incorporating nonlinear prey refuge under the influence of fear effect and additional food // Journal of Physics A: Mathematical and Theoretical. — 2020. — Vol. 53, No. 29. — 295601. — https://doi.org/10.1088/1751-8121/ab81d8

Nabti A., Ghanbari B. Global stability analysis of a fractional SVEIR epidemic model // Mathematical Methods in the Applied Sciences. — 2021. — Vol. 44, No. 11. — P. 8577–8597.

Pal S., Majhi S., Mandal S., Pal N. Role of fear in a predator – prey model with Beddington – DeAngelis functional response // Zeitschrift Fur Naturforschung – Section A Journal of Physical Sciences. — 2019. — Vol. 74, No. 7. — https://doi.org/10.1515/zna-2018-0449

Pal S., Pal N., Chattopadhyay J. Hunting cooperation in a discrete-time predator – prey system // International Journal of Bifurcation and Chaos. — 2018. — Vol. 28, No. 7. — https://doi.org/10.1142/S0218127418500839

Pal S., Panday P., Pal N., Misra A.K., Chattopadhyay J. Dynamical behaviors of a constant prey refuge ratio-dependent prey – predator model with Allee and fear effects // International Journal of Biomathematics. — 2024. — Vol. 17, No. 01. — 2350010. — https://doi.org/10.1142/S1793524523500109

Rohith G., Devika K.B. Dynamics and control of COVID-19 pandemic with nonlinear incidence rates // Nonlinear Dynamics. — 2020. — Vol. 101, No. 3. — P. 2013–2026. — https://doi.org/10.1007/s11071-020-05774-5

Sasmal S.K. Population dynamics with multiple Allee effects induced by fear factors — A mathematical study on prey – predator interactions // Applied Mathematical Modelling. — 2018. — Vol. 64. — P. 1–14. — https://doi.org/10.1016/j.apm.2018.07.021

Sen D., Ghorai S., Banerjee M. Allee effect in prey versus hunting cooperation on predator-enhancement of stable coexistence // International Journal of Bifurcation and Chaos. — 2019. — Vol. 29, No. 6. — https://doi.org/10.1142/S0218127419500810

Shang Z., Qiao Y. Bifurcation analysis in a predator – prey model with strong Allee effect on prey and density-dependent mortality of predator // Mathematical Methods in the Applied Sciences. — 2024. — Vol. 47, No. 4. — P. 3021–3040. — https://doi.org/10.1002/mma.9793

Thirthar A. A., Majeed S. J., Alqudah M. A., Panja P., Abdeljawad T. Fear effect in a predator – prey model with additional food, prey refuge and harvesting on super predator // Chaos, Solitons & Fractals. — 2022. — Vol. 159. — 112091. — https://doi.org/10.1016/j.chaos.2022.112091

Vinoth S., Sivasamy R., Sathiyanathan K., Unyong B., Rajchakit G., Vadivel R., Gunasekaran N. The dynamics of a Leslie type predator – prey model with fear and Allee effect // Advances in Difference Equations. — 2021. — Art. 338. — https://doi.org/10.1186/s13662-021-03490-x